# Selective Reactivity of the Phosphorus−Chlorine and Carbon−Chlorine Bonds in Cyclic Chlorocarbaphosphazenes: An Unusual Activation of a Carbon−Nitrogen Bond in Trialkylamines†

**Ashwani Vij, Anil J. Elias,‡ Robert L. Kirchmeier, and Jean'ne M. Shreeve***

Department of Chemistry, University of Idaho, Moscow, Idaho 83844-2343

*Received October 24, 1996*⊗

Acyclic tertiary amines such as triethylamine and tri-*n*-propylamine used as HCl scavengers in nucleophilic substitution reactions of cyclic chlorocarbaphosphazenes [$N_3PC_2Cl_4$ (**I**) and $N_3P_2CCl_5$ (**II**)] with $(CF_2)_n(CF_2CH_2OH)_2$ [$n = 0$ (**III**) or 1 (**IV**)] are found to undergo a facile C−N bond cleavage with the regiospecific substitution of the dialkylamino groups on the ring carbon atoms of the carbaphosphazene. In the case of cyclic amines such as 1-methylpiperidine and 4-methylmorpholine, the cleavage was found to occur regiospecifically at the N−$CH_3$ bond, resulting in the ring substitution of the cyclic secondary amino group on the dicarbaphosphazene ring carbon atoms. The polyfluoro diol **III** forms a spirocyclic ring exclusively at the phosphorus site in compounds $[CF_2CH_2O]_2PN_3C_2[N(C_2H_5)_2]_2$ (**1**), $[CF_2CH_2O]_2PN_3C_2[N(C_3H_7)_2]_2$ (**2**), $[CF_2CH_2O]_2PN_3C_2[NCH_2(CH_2)_3CH_2]_2$ (**3**), and $[CF_2CH_2O]_2PN_3C_2[N(CH_2)_2O(CH_2)_2]_2$ (**5**) along with the formation of carbon-substituted carbaphosphazenes, $Cl_2PN_3C_2[NCH_2(CH_2)_3CH_2]_2$ (**4**) and $Cl_2PN_3C_2[N(CH_2)_2O(CH_2)_2]_2$ (**6**). Reaction of **II** with **III** in the presence of triethylamine affords the dispiro product $[CF_2CH_2O)_2]_2P_2N_3C[N(C_2H_5)_2]$ (**7**), which crystallizes in a polar orthorhombic space group, $Cmc2_1$. Upon refluxing of **I** or **II** with $R_3N$ (R = $C_2H_5$, *n*-$C_3H_7$) in toluene, the amino-substituted carbaphosphazenes, $Cl_2PN_3C_2[N(C_2H_5)_2]_2$ (**8**), $Cl_4P_2N_3C[N(C_2H_5)_2]$ (**9**), and $Cl_4P_2N_3C[N(n\text{-}C_3H_7)_2]$ (**10**) are obtained in good yields. Hydrolysis of **8** leads to the formation of $Cl(O)PN(H)N_2C_2[N(C_2H_5)_2]_2$ (**11**). When lithium salts of the fluoro diols **III** and **IV** are reacted with **I** or **II** in diethyl ether, the P−Cl bond is selectively substituted, yielding the spirocyclic $[CF_2CH_2O]_2PN_3C_2Cl_2$ (**12**), $[CF_2(CF_2CH_2O)_2]PN_3C_2Cl_2$ (**13**), $[CF_2CH_2O]_2P_2N_3CCl_3$ (**14**), and $[(CF_2CH_2O)_2]_2P_2N_3CCl$ (**15**). The C−Cl bonds in **12** and **14** were easily substituted by their reaction with 4-$FC_6H_4XNa$ (X = O or S) to form $[CF_2CH_2O]_2PN_3C_2[4\text{-}FC_6H_4O]_2$ (**16**) and $[CF_2CH_2O]_2PN_3C_2[4\text{-}FC_6H_4S]_2$ (**17**). Reactions of **12** and **13** with $(CH_3)_3SiN(CH_3)_2$ under mild conditions result in the elimination of $(CH_3)_3SiCl$ along with the formation of $[CF_2CH_2O]_2PN_3C_2[N(CH_3)_2]_2$ (**18**). The X-ray analyses of **13** and **18** represent the first examples of eight-membered spirocyclic phosphazenes. The thermal behavior of **II**, **9**, **10, 14**, and **15** has also been investigated at 120 °C. Single-crystal X-ray diffraction studies were carried out for **1**, **2**, **7**, **9**−**14**, and **16**−**19**, and these compounds are also characterized using IR, $^1H$, $^{13}C$, $^{19}F$ and $^{31}P$ NMR spectroscopy, MS, and elemental analysis.

## Introduction

The chemistry of cyclic triphosphazenes has been a subject of extensive investigation.[1−5] These compounds are known to undergo thermal ring expansion or ring opening polymerization behavior.[1,6] Cyclic carbaphosphazenes $[NPX_2]_n[NCX]_{3-n}$ ($n$ = 1, 2; X = R, Cl, OR, $NR_2$, SR, etc.) form an important class of compounds whose structures, properties, and reaction behavior can be linked to both *s*-triazenes[7,8] and cyclic phosphazenes[1] as they contain both P−N and C−N moieties as part of the ring structure. The presence of a carbon atom in the PNC heterocycle renders different properties to these compounds. For example, in contrast to the high temperature/time requirement for the thermal ring opening polymerization of $N_3P_3Cl_6$, ∼250 °C,[9] $N_3P_2CCl_5$ can be easily polymerized at 120 °C/3−4 h to form the linear polymer[10] $-[C(Cl)=NP(Cl)_2=NP(Cl)_2=N-]_n$. On the other hand, perfluoroalkyl-substituted dicarbaphosphazenes of the type $[R_fCN]_2[R_2PN]$ [$R_f$ = perfluoroalkyl, perfluoroalkoxy] show high thermal stability and, therefore, find applications as additives for controlling and arresting oxidation and degradation of polyfluoroalkyl ether high-temperature lubricants and fluids.[11−14] The nature of these compounds complements some high molecular weight fluoro polyethers which are currently being investigated in our laboratories for

† Presented at the 211th National Meeting of the American Chemical Society, New Orleans, LA, March 24−29, 1996; Abstr. INOR 613.

‡ Summer faculty research participant. Department of Chemistry, Indian Institute of Technology, Kanpur, India 208 016.

⊗ Abstract published in *Advance ACS Abstracts,* May 1, 1997.

(1) Allcock, H. R. *Phosphorus-Nitrogen Compounds*; Academic Press: New York, 1972 and references therein.
(2) Shaw, R. A. *Pure Appl. Chem.* **1980**, *52*, 1063 and references therein.
(3) Labarre, J. F. *Top. Curr. Chem.* **1985**, *129*, 173 and references therein.
(4) Shaw, R. A. *Phosphorus Sulfur Relat. Elem.* **1986**, *28*, 203 and references therein.
(5) Chandrasekhar, V.; Murlidhara, M. G. R.; Selvaraj, I. I. *Heterocycles* **1990**, *31*, 2231 and references therein.
(6) *Inorganic and Organometallic Polymers II: Advanced Materials and Intermediates*; Wisian-Neilson, P., Allcock, H. R., Wynne, K. J., Eds.; ACS Symposium Series 572; American Chemical Society: Washington, DC, 1994 and references therein.
(7) Smolin, E. M.; Rapoport, L. *s-Triazines and Derivatives*, Interscience: New York, 1967.
(8) Qirke, J. M. E 1,3,5-Triazines. In *Comprehensive Heterocyclic Chemistry*, Vol. 3, Part 2B; Boulton, A. J., Haubold, W., Eds.; Pergamon Press: New York, 1972.
(9) Mark, J. E.; Allcock, H. R.; West, R. C. *Inorganic Polymers*; Prentice Hall: Englewood Cliffs, NJ, 1992; Chapter 3.
(10) Allcock, H. R.; Coley, S. H.; Manners, I.; Visscher, K. B.; Parvez, M.; Nuyuken, O.; Renner, G. *Inorg. Chem.* **1993**, *32*, 5088 and references therein.
(11) Pacioreck, K. J. L. US Patent US 601,874, 26 Oct 1984; (*Chem. Abstr.* **1985**, *102*, 116423.
(12) Pacioreck, K. J. L. US Patent US 865, 271, 23 June 1978; (*Chem. Abstr.* **1979**, *90*, 138014.
(13) Pacioreck, K. J. L.; Ito, T. I.; Nakahara, J. H.; Harris, D. H.; Kratzer, R. H. *J. Fluorine Chem.* **1983**, *22*, 185.
(14) Pacioreck, K. J. L.; Ito, T. I.; Kratzer, R. H. *Sci. Tech. Aerosp. Rep.* **1982**, *20*, N82, 12135.

S0020-1669(96)01292-X CCC: $14.00 

similar purposes.[15] The difference in the chemistry of these carbaphosphazenes is also reflected by the fact that while the alkoxy/fluoroalkoxy-substituted cyclotriphosphazenes and polytriphosphazenes are hydrolytically stable, their carbaphosphazene counterparts result in degradation when exposed to moisture.[10] Further, carbaphosphazenes offer two different reactive sites for substitution, at the C−Cl and P−Cl bonds, which show preferential reactivities according to the nature of nucleophiles employed in these reactions.[16,17] In continuation of our studies on the chemistry of poly(fluoroalkoxy)- and poly((fluoroaryl)oxy)-substituted fluorophosphazenes,[18,19] we now report a detailed synthetic and structural investigation of the carbaphosphazene chemistry. Trialkylamines have been widely used as effective hydrogen halide scavengers in the reactions of cyclotriphosphazenes with alcohols.[1,20] However, in this study we find that these tertiary amines undergo facile C−N bond cleavage followed by the regioselective substitution of the C−Cl bonds in the carbaphosphazene rings.

## Results and Discussion

The presence of two different reactive sites in $N_3P_2CCl_5$ (**I**) and $N_3PC_2Cl_4$ (**II**), namely, the P−Cl and C−Cl bonds, provides a variety of synthetic possibilities. In **I** and trichlorodicarbaphosphazenes[21] the C−Cl bond reacts preferentially with amines or silylamines.[22,23] These reactions generally proceed with a stepwise substitution of the chlorine atoms with the initial reactions on the C−Cl bonds. However, an excess of amines or trimethylsilylamine is found to substitute all of the chlorine atoms to give tetrakis(amino) derivatives. On the other hand, the P−Cl bond shows selectivity with metal alkoxides, but the yield of the 2,2,2-trifluoroethoxy-substituted dicarbaphosphazene is quite low under the conditions employed for its synthesis.[16] The chemistry of monocarbaphosphazenes has been explored with secondary amines[24−26] and Grignard reagents[24] and resulted in the formation of C-substituted (ring carbon substitution by amino or alkyl/aryl groups) or pentakis(amino)-substituted products. Reactions of **II** and C-alkyl/aryl- and C-amino-substituted monocarbaphosphazenes with alkoxides are also described,[10,27] and reactions of alkyl-substituted dicarbaphosphazenes are reported with nitrogen-, oxygen-, and sulfur-containing bifunctional nucleophiles.[28]

In this study, the reaction of the diol $[CF_2CH_2OH]_2$ (**III**) with $N_3PC_2Cl_4$ in the presence of triethyl- and tri-*n*-propylamine results not only in the formation of a seven-membered spirocycle on the phosphorus atom but also in the substitution on the carbon atoms by dialkylamino groups as shown in Scheme 1 However, if cyclic tertiary amines such as 1-methylpiperidine and 4-methylmorpholine are employed as HCl scavengers, the N-$CH_3$ bond in these amines is selectively activated to form the spirocyclic carbaphosphazenes, **3** and **5**, in addition to a minor amount of C-amino-substituted chlorocarbaphosphazenes, **4** and **6** (Scheme 2).

**Scheme 1**

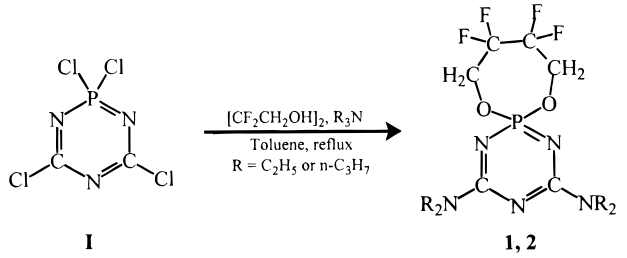


**I** **1, 2**

**Scheme 2**

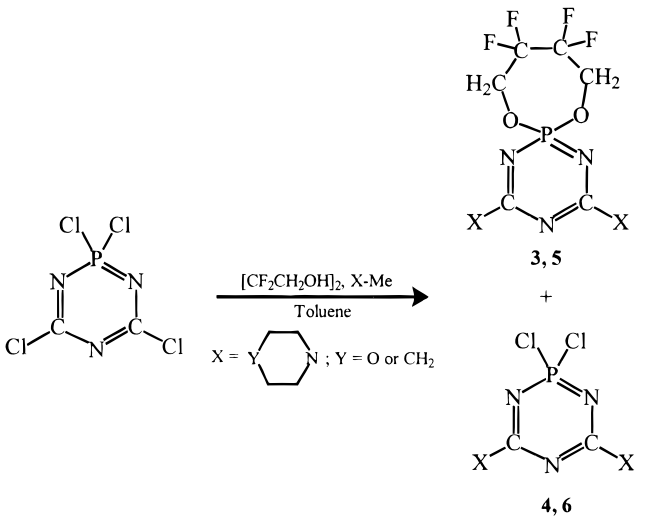


**3, 5** + **4, 6**

Similarly the reaction of **II** with 2 equiv of $[CF_2CH_2OH]_2$ proceeds smoothly in the presence of triethylamine to form the dispiro monocarbaphosphazene **7**, with a diethylamino group substituted on the carbon atom.

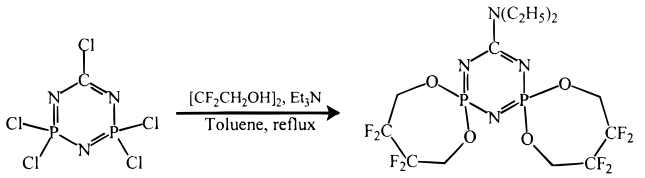


**II** **7**

The compounds **1**, **2**, **3**, **5**, and **7** show greater air/moisture stability than $N_3PC_2Cl_4$ and are readily isolated from their reaction mixtures. In all reactions involving **II**, amine, and $[CF_2CH_2OH]_2$, traces of the dichloro derivative, $[R_2N]_2C_2N_3PCl_2$, are also identified but not separated from the polymeric residue. The $^1$H NMR spectra of the compounds **1**, **2**, **3**, **5**, and **7** show a multiplet for the $OCH_2$ group in the range 4.32−4.38 ppm. The $NCH_2$ protons of the dialkylamino groups are significantly deshielded (1.2−1.3 ppm) *vis-à-vis* the free amines. The $^{19}$F NMR spectra of these compounds show a resonance at ∼ −127.6 ppm, characteristic for a seven-membered spirocyclic 3,3,4,4-tetrafluorobutanedioxy group on a pentavalent phosphorus site.[18] The $^{31}$P signal for the spirocyclic phosphorus atom in **1**, **2**, **3**, or **5** appears at ∼40.0 ppm as a pseudopentet (a singlet in the $^{31}P\{^1H\}$ NMR spectrum) that arises from coupling with the protons of the spirocyclic $(OCH_2CF_2)_2$ groups ($^3J_{P-H}$ = 16.3 Hz). The $^{13}$C chemical shift of the ring NCN carbon atom is very useful in differentiating an amino-substituted ring carbon atom (164 ppm) from a chloro-substituted ring carbon atom (172 ppm).[16] A characteristic doublet pattern for the ring carbon atoms is seen in the range 163.2−165.2 ppm ($^2J_{C-P}$ = 11.3

(15) Krumm, B.; Vij, A.; Kirchmeier, R. L.; Shreeve, J. M. *Inorg. Chem.* **1997**, *36*, 366.
(16) Roesky, H. W.; Mainz, B. *Z. Anorg. Allg. Chem.* **1986**, *540/541*, 212.
(17) Schmidpeter, A.; Schindler, N. *Chem. Ber.* **1968**, *101*, 2602.
(18) Elias, A. J.; Kirchmeier, R. L.; Shreeve, J. M. *Inorg. Chem.* **1994**, *33*, 2727.
(19) Vij. A.; Geib, S. J.; Kirchmeier, R. L.; Shreeve, J. M. *Inorg. Chem.* **1996**, *35*, 2915.
(20) Allcock, H. R.; Turner, M. L.; Visscher, K. B. *Inorg. Chem.* **1992**, *31*, 4354.
(21) Fischer, E.; Weber, Heike; Michalik, M. *Z. Chem.* **1981**, *21*, 137.
(22) Pinkert, W.; Schoening, G.; Glemser, O. *Z. Anorg. Allg. Chem.* **1977**, *436*, 136.
(23) Fluck, E.; U. Pachali, *Chem.-Ztg.* **1982**, *106*, 270.
(24) Schmid, E.; Fluck, E. *Z. Naturforsch.* **1977**, *32b*, 254.
(25) Schmidpeter, A.; Schindler, N. *Chem. Ber.* **1969**, *102*, 856.
(26) Schmidpeter, A.; Schindler, N. *Z. Anorg. Allg. Chem.* **1969**, *367*, 130.
(27) Schmidpeter, A.; Schindler, N. *Z. Anorg. Allg. Chem.* **1970**, *372*, 214.
(28) Kornuta, P. P.; Kolotilo, N. V.; Markovskii, L. N. *Zh. Obshch. Khim.* **1982**, *52*, 2742.

Hz) for the compounds described above. The $CF_2$ group appears at ~113 ppm as a triplet of triplets due to one- and two-bond carbon−fluorine couplings ($^1J_{C-F}$ = ~255 Hz, $^2J_{C-F}$ = ~25 Hz). For the C-amino-substituted carbaphosphazenes with a $PCl_2$ moiety, the $^{31}$P NMR chemical shift (57.5 ppm) is quite similar to that of **II** (55.6)[29] whereas the ring carbon resonates upfield at 163−164 ppm with a smaller $^2J_{C-P}$ coupling constant of ~8.5 Hz. In the case of $[CF_2CH_2O)_2]_2P_2N_3C[N(C_2H_5)_2]$ (**7**), the $^{31}$P NMR spectrum shows a signal at 28.4 ppm.

The activation of a C−N bond in trialkylamines is both interesting and unexpected as the conditions employed in this study are quite mild compared to the analogous reactions with aromatic and heteroaromatic halides. In the latter case, halogen replacement by a secondary amino group takes place at very high pressures of 0.8 kPa and 100 °C over a period of 4 days.[30] To the best of our knowledge this is the first time such a reaction has been reported for a cyclic carbaphosphazene.

Upon reacting **I** or **II** with a large excess of $R_3N$ (about an 8-fold excess, R = $C_2H_5$ or $C_3H_7$, **8**−**10**), the dialkylamino group is substituted selectively at the carbon atom(s) with the P−Cl bonds remaining unchanged. The side product of these reactions is trialkylammonium hydrochloride as characterized by $^1$H and $^{13}$C NMR spectra. Extraction of the reaction product with hexane is an easy way to eliminate the ammonium salt and the C-amino-substituted carbaphosphazenes, which can be further purified by recrystallization or vacuum sublimation. The

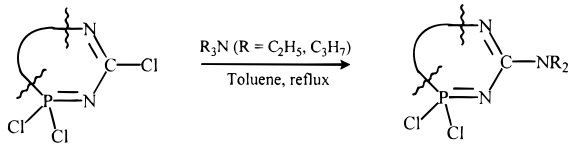


formation of trialkylamine hydrochloride as the only identifiable byproduct in these reactions indicates that the eliminated alkyl group likely undergoes E2 elimination of HCl and ethylene. The HCl produced reacts with the excess triethylamine in the reaction mixture, yielding the amine hydrochloride. The observation of a polymeric side product also supports the proposed mechanism as shown. This reaction also shows considerable similarity to the von Braun cyanogen bromide reaction, where tertiary amines can be converted to secondary amines.[31]

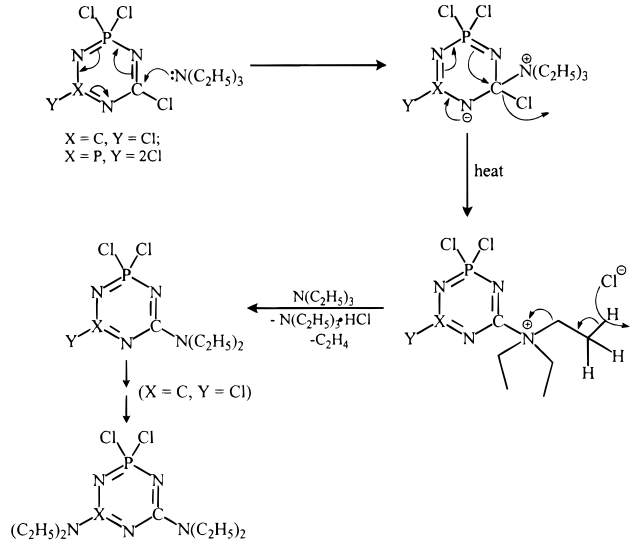


The C−$NR_2$ substituted carbaphosphazenes are moisture sensitive, and on extended exposure to laboratory air, one of the P−Cl bonds is hydrolyzed. The presence of a strong band in the infrared spectrum at 1252 ($\nu_{P=O}$) and a broad band at 3400 ($\nu_{NH}$) $cm^{-1}$ supports the proposed derivative, **11**.

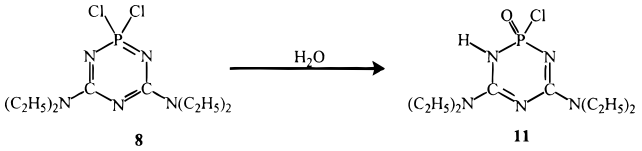


The appearance of an NH proton in the $^1$H NMR spectrum as a very broad peak at 9.23 ppm is suggestive of some intra- or intermolecular hydrogen bonding. The $^{31}$P NMR spectrum shows an upfield shift of the resonance from 36.1 in **9** to 10.9 ppm, which also suggests the formation of cyclic carbaphosphorin **11**. Due to the presence of a proton on the ring nitrogen atom, the diethylamino groups show magnetic inequivalence in the $^{13}$C NMR spectrum. Two sets of signals are observed for the $CH_3$ and $CH_2$ groups of the $N(CH_2CH_3)_2$ moiety, as well as an overlapping set of doublets for the ring carbons at 151.66 and 151.71 ($^2J_{C-P}$ = 3.6 Hz).

Selective substitution of the P−Cl bond is achieved by employing stoichiometric amounts of bis(lithium fluoroalkoxides). This is similar to the method reported by Roesky,[16] but much higher yields of the reaction products were obtained in this study. This may be attributed to the generation of the lithium salt *in situ*, the use of diethyl ether as a solvent, and the use of milder reaction conditions.

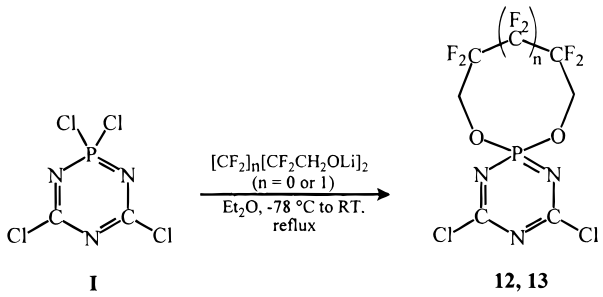


Purification of the crude product by vacuum sublimation provided an excellent source of X-ray diffraction quality crystals. A polymeric residue left after sublimation could not be characterized. In these reactions, we were unable to detect any substitution of the C−Cl bond, suggesting that ionic reagents preferentially attack the P−Cl bond. The $^{31}$P NMR spectra for these derivatives shows a pseudopentet resonance ~28 ppm ($^3J_{P-H}$ = 15.5−17.6 Hz). The position of the $^{13}$C chemical shift for the phosphazene ring carbon atom, ~172.3 ppm, is similar to that reported for **I** and its $OCH_2CF_3$ derivative,[16] supporting substitution exclusively at the phosphorus atom.

If an analogous reaction is carried out by using stoichiometric amounts of **II** and **III**, a mixture of both a monospiro, $[CF_2CH_2O]_2P_2N_3CCl_3$ (**14**), and a dispiro carbaphosphazene, $[(CF_2CH_2O)_2]_2P_2N_3CCl$ (**15**), is formed. The $^{31}$P NMR spectrum allows the easy identification of **14** and **15** as the former shows two resonances at 17.3 (doublet of pentets, $^3J_{P-H}$ = 16.8 Hz, $^3J_{P-P}$ = 67.3 Hz) and a doublet at 40.9 ppm attributable to $P_{spiro}$ and $P_{dichloro}$ phosphorus atoms, respectively, while the latter shows a multiplet at 22.7 ppm. The $^{13}$C NMR spectrum shows two narrowly spaced triplets at 168.8 (tentatively assigned to

(29) Becke-Goehring, M.; Jung, D. *Z. Anorg. Allg. Chem.* **1970**, *372*, 233.
(30) Matsumoto, K.; Hashimoto, S.; Otani, S. *J. Chem. Soc., Chem. Commun.* **1991**, 306.
(31) Hageman, H. A. The von Braun cyanogen bromide reaction. In *Organic Reactions, Vol. VII*; Blatt, A. H., Cope, A. C., McGrew, F. C., Niemann, C., Snyder, H. A., Eds.; John Wiley: New York, 1953; p 198.

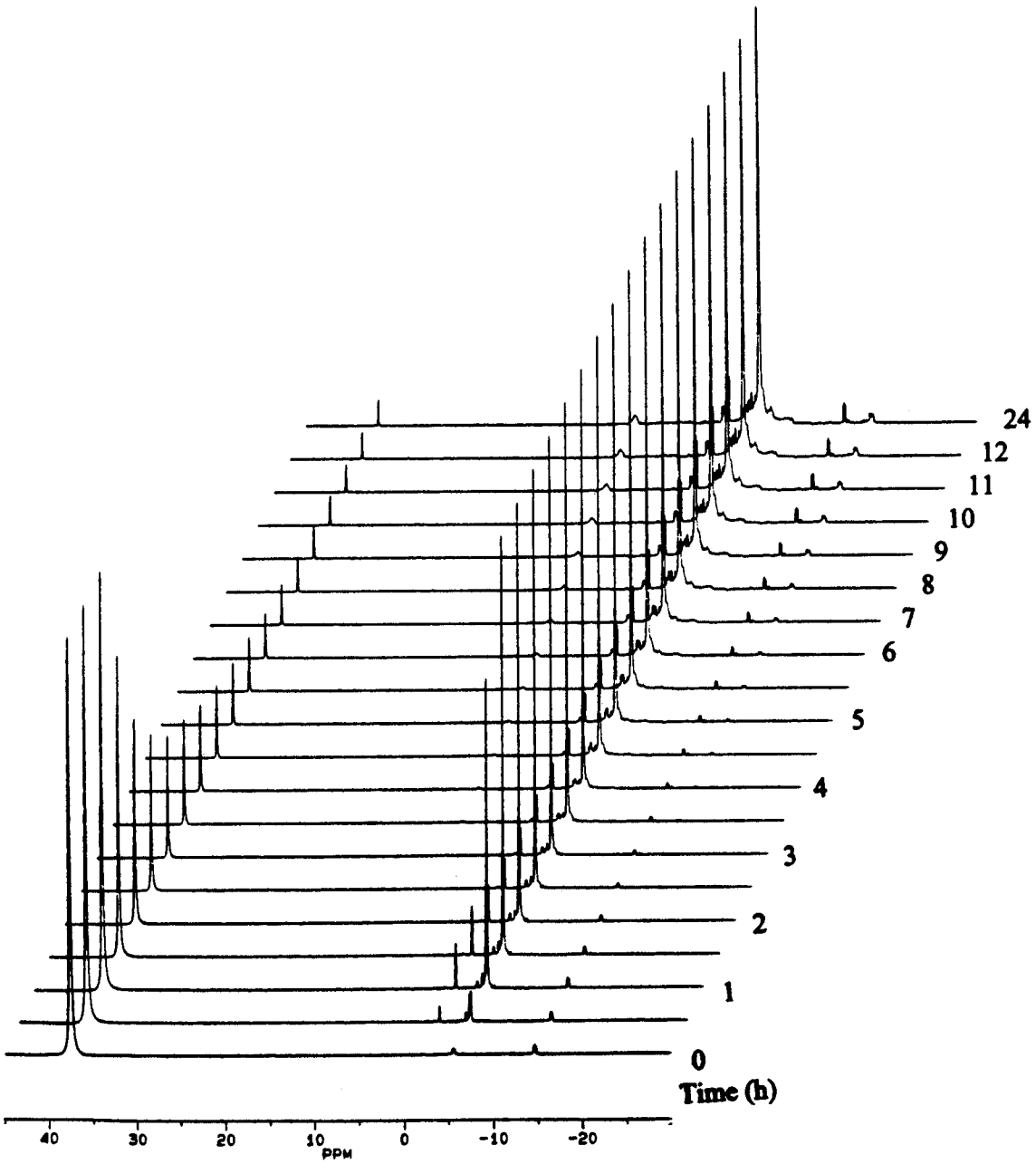


**Figure 1.** Instability of monocarbaphosphazene monitored by $^{31}P$ NMR.

**15**) and 170.0 ppm with $^2J_{C-P} = 15.2$ and 15.0 Hz, respectively. The dispiro derivative is formed as 25−30% of the total yield as determined from the relative integration values in the $^{31}P$ NMR spectrum. Variation of the reaction stoichiometry is not useful for increasing the yield of the monospiro product. If the sodium salt of **III** is used in the synthesis, the formation of the dispiro derivative is attenuated (∼10% yield), but there are numerous other resonances, probably due to the attack at the C−Cl bond. Further, our attempts to separate these derivatives by slow sublimation were not successful. However, **14** sublimed as a colorless crystalline solid while **15** remained amorphous.

### Substitution Reactions of Spirocyclic Chlorocarbaphosphazenes

The residual chlorine atoms on the carbaphosphazene ring react with sodium phenoxide/thiophenoxide in diethyl ether under mild conditions to form spirocyclic dicarbaphosphazenes containing an arylether or arylthioether functionality. The spirocyclic carbaphosphazene **12** was used as a model reagent to investigate the substitution reactions and determine the stability of these fully substituted carbaphosphazenes.

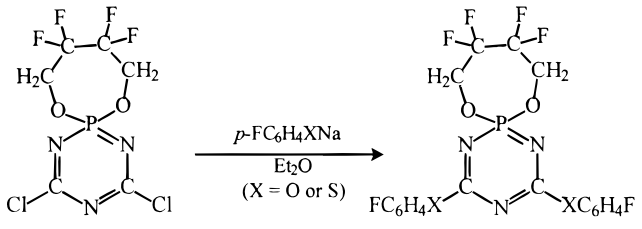


**12** **16 (X = O), 17 (X = S)**

Both compounds are obtained as crystalline solids (∼80% yield) following recrystallization from a chloroform/hexane mixture. Substitution of the C−Cl bonds in $N_3PC_2(C_6H_5)Cl_3$ with $C_6H_5SNa$ has been described, but the thiophenoxy-substituted chlorocarbaphosphazene could not be isolated.[32] The EI mass spectral data for **16** does not show a parent ion peak as observed for **17**. The highest *m/e* peak observed (also the base peak) corresponds to the loss of a *p*-fluorophenoxy group.

(32) Kornuta, P. P.; Kolotilo, N. V.; Markovskii, L. N. *Zh. Obshch. Khim.* **1982**, *52*, 590.

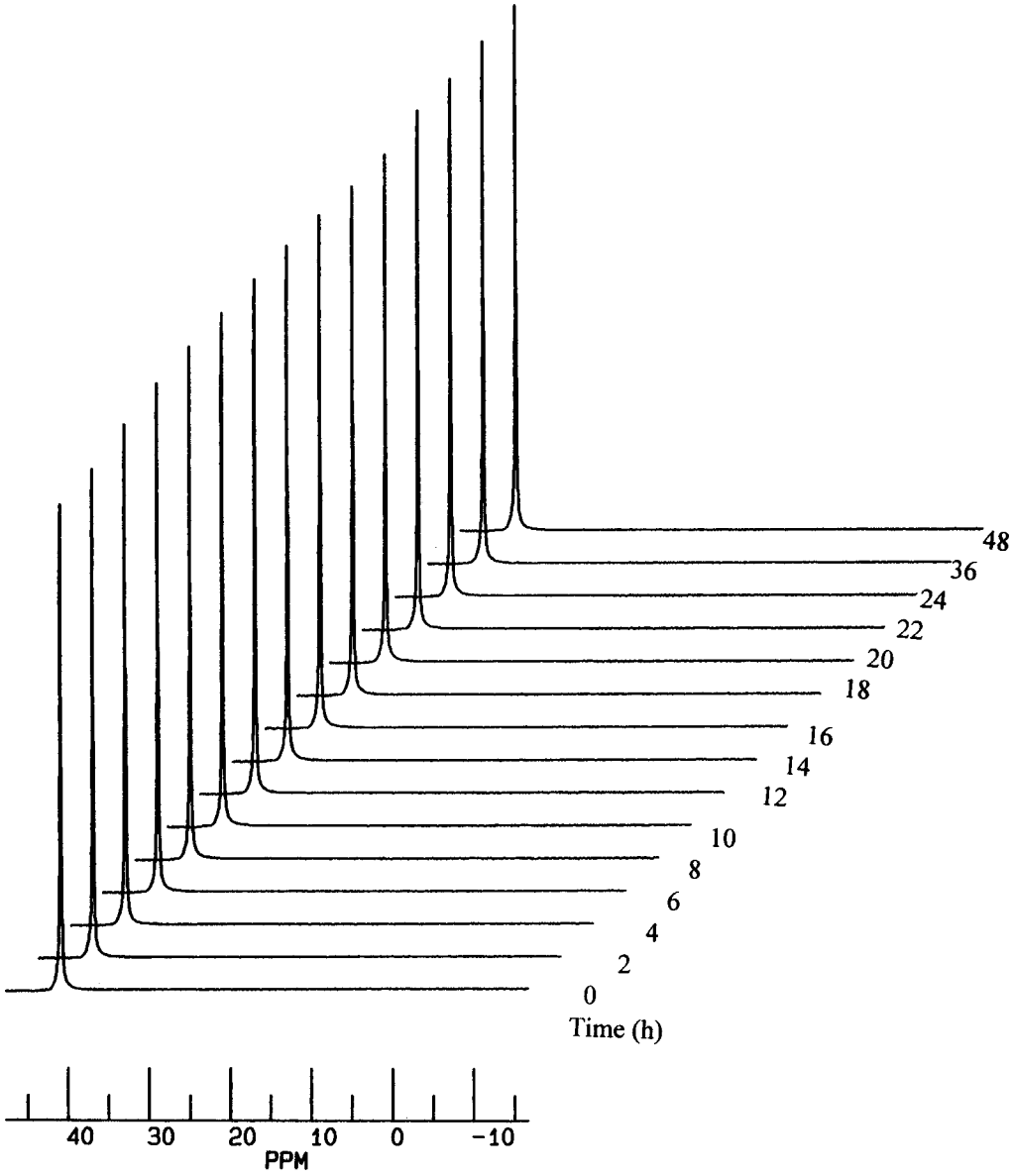


**Figure 2.** Thermal stability of amino-substituted monocarbaphosphazene monitored by $^{31}P$ NMR.

However, the CI mass spectrum shows a peak at *m/e* = 480, which corresponds to $M^+ + 1$. The $^{31}P$ NMR shows a pseudopentet resonance ($^3J_{P-H} = 17.2$ Hz) at 42.7 and 26.7 ppm for **16** and **17**, respectively. For spiro-2,2,3,3-tetrafluorobutanedioxy-substituted dicarbaphosphazenes, the position of the $^{31}P$ NMR shift depends upon the substituent at the carbon atoms and follows the order (increasing upfield shift) C−$OC_6H_4F$-*p* > C−$NR_2$ > C−Cl > C−$SC_6H_4F$-*p*.

Reactions of **12** and **13** with $Me_3SiN(CH_3)_2$ in refluxing $CH_2Cl_2$ substitute the Cl atoms with $N(CH_3)_2$ groups, affording **18** and **19** in 85−90% yield.

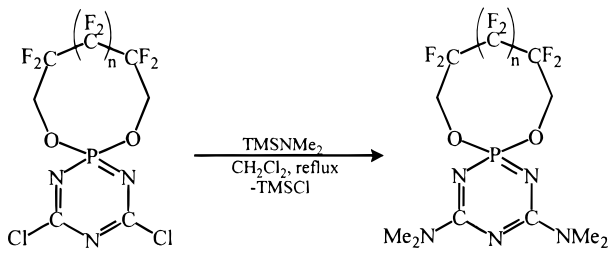


**12, 13** **18, 19**

In **18** and **19** the $^{31}P$ NMR resonance at ∼40 ppm shows a lower $^3J_{P-H}$ value of 15.2 Hz compared to that for the oxygen/sulfur-substituted carbaphosphazenes **16** and **17**. An upfield shift of the $^{13}C$ NMR resonance from ∼172 in the parent compounds **12** and **13** to 165.8 ppm is accompanied by an increase in the $^2J_{C-P}$ value from 11.2 Hz to 18.2 Hz in these derivatives. The mass spectra for both **18** and **19** show parent ions as the base peaks in the EI/MS. Subsequent peaks result from the loss of a $CH_3$ and $N(CH_3)_2$ fragments.

## Thermal Behavior of Monocarbaphosphazenes

Dicarbaphosphazene derivatives are known to exhibit high thermal stability. On the other hand, monocarbaphosphazene **II** undergoes rapid thermal ring opening at 120 °C.[33] A study of the polymerization behavior as a function of time and temperature has also been reported recently.[10] We have also carried out some experiments to explore the thermal behavior of a few substituted monocarbaphosphazenes. The progress of the polymerization of **II** was monitored on-line at 120(0.1) °C in a preheated probe by using $^{31}P$ NMR spectroscopy. An analysis of the FID data acquired initially at intervals of 10 min for 2 h, followed by intervals of 20 min for the next 3 h and finally intervals of 1 h until the completion of the 24 h

(33) Allcock, H. R.; Coley, S. H.; Manners, I.; Visscher, K. B.; Parvez, M.; Nuyuken, O.; Renner, G. *Macromolecules* **1991**, *24*, 2024.

experiment, shows that most of the decomposition takes place within the first 4 h (Figure 1), as suggested by Allcock.[10] A small amount of the cyclic trimer remains even after prolonged heating. In contrast to this, the amino-substituted carbaphosphazenes show remarkable thermal stability as shown by a $^{31}P$ NMR experiment at 120 °C analogous to that described above. No change in the $^{31}P$ NMR chemical shift/intensity is noticed and the trimer is recovered even after heating at 120 °C for 48 h (Figure 2). Attempts to ring-open by the addition of Lewis acids such as $SnCl_4$ are not successful. However, addition of sulfamic acid in the presence of calcium sulfate dihydrate results in ring degradation, suggested by a decrease in the intensity of the $^{31}P$ peak at 40 ppm accompanied by a gradual growth of three other peaks in the 5 to −20 ppm region. The viscous mixture becomes a solid mass after prolonged heating, probably with the formation of a cross-linked polymer.

In monocarbaphosphazenes the ring opening can take place by the cleavage of P−N, C−N, or both of these bonds. The mechanism proposed for the thermal ring opening of $N_3P_3Cl_6$ suggests that a P−halogen bond is an essential requirement for the melt polymerization process.[20] If this is also true for carbaphosphazenes, substitution of the C−Cl bond with $C-N(C_2H_5)_2$ groups should have little or no influence on the polymerization behavior of **9**. In fact, the presence of the C−Cl moiety is essential for polymerization in our experience. In order to get additional support for this observation, we carried out a high-temperature (120 °C) $^{31}P$ NMR experiment for **10** and a mixture of **14** and **15**. Compound **10** shows a thermal behavior similar to that of **9**, indicating that chain length does not alter polymerization behavior. Compound **14** contains both a P−Cl and a C−Cl bond whereas **15** contains only a C−Cl bond. After a period of 8 h, peaks at 17.3 and 40.9 ppm due to **14** begin to decrease in intensity with respect to the peak at 22.7 assigned to the $P_{spiro}$ in **15**, and they ultimately disappear after about 24 h. Concomitantly, a very broad hump appears at ∼−4 ppm which may be due to the higher oligomers or polymeric material. These results suggest that, in the absence of a P−Cl bond, the monocarbaphosphazene derivatives are thermally stable, which implies that both C−Cl and P−Cl bonds are involved in the ring-opening process.

The thermal stability of amino-substituted monocarbaphosphazenes **9** and **10** is very intriguing. While $N_3P_2CCl_5$ undergoes almost complete thermal ring opening polymerization within 5 h at 120 °C, the $N(C_2H_5)_2$- or $N(C_3H_7)_2$-substituted monocarbaphosphazenes exhibit marked thermal stability. In order to make a meaningful comparison, we carried out the data collection for **9** and **10** as well as **II**[34] at 193 K. Previous attempts to obtain low-temperature crystal data for **II** were unsuccessful due to crystal decomposition.[10] However, the availability of a diffractometer equipped with a CCD area detector enabled us to carry out rapid data collection for about 6 h without any crystal decomposition. The gross structural features are similar to those reported by Allcock. Both **9** (Figure 3) and **10** (Figure 4) contain a slightly distorted $N_3P_3C$ core with mean deviations of 0.022 and 0.026 Å, respectively, with P1 = −0.041 and N1 = 0.036 Å from the mean plane. Substitution of the chlorine atom on the ring carbon atom in **II** with a dialkylamino group results in the formation of a short exocyclic C1−N4 bond [1.356(5) Å in **9**; 1.341(2) Å in **10**] (Tables 1−5and 6) and $\pi$-electron density mobilization toward the $N_3P_2C$ ring. This polarizing effect causes an increase in the endocyclic C−N bonds and C−N−P angles from 1.324(4) Å (average) and ∼118° in **II** to 1.360(4) Å and ∼120.4° in **9** and **10**. Consequently, the N−C−N angles decrease from 133.1(3)° to ∼127.4(4)° upon substitution. This implies that the presence of an electronegative group on the carbon atom will enhance thermal ring opening while electron-releasing groups make the ring thermally stable. Further investigation of the thermal behavior of various C- as well as P-substituted monocarbaphosphazenes is currently in progress in our laboratories.

(34) The structure of **II** was determined at 193 K. The data collection parameters are listed in Table 1c. Bond lengths and bond angles are quite similar to those reported in ref 10 and available as Supporting Information.

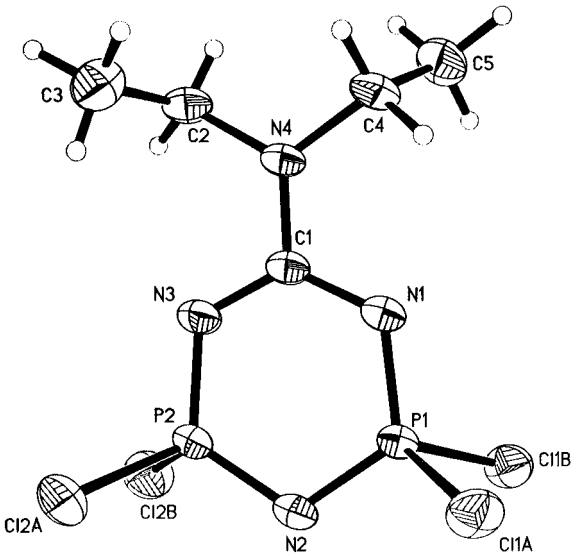


**Figure 3.** X-ray crystal structure of **9**.

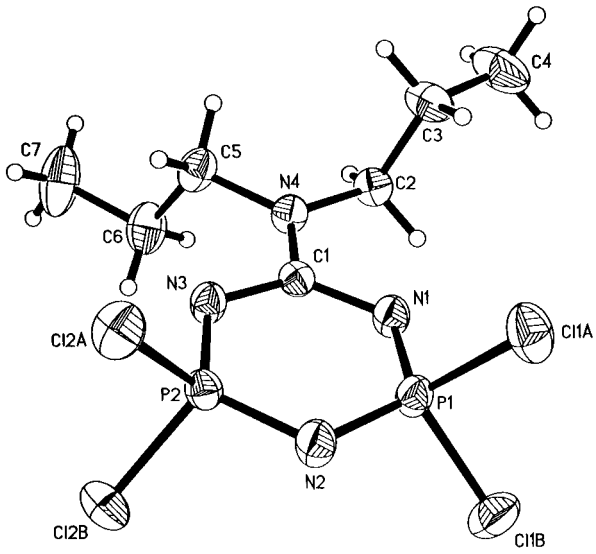


**Figure 4.** X-ray crystal structure of **10**.

## X-ray Diffraction Studies

A survey of the Cambridge Crystal Structure Database (CCSD)[35] reveals that only about a dozen carbaphosphazenes have been structurally characterized. These include structures for six-membered monocarbaphosphazenes[10,36−39] and dicarbaphosphazenes[40−45] as well as an eight-membered[46] and twelve-membered[47] carbaphosphazene derivatives. However, there are no structures known for spirocyclic carbaphosphazenes containing a nitrogen, oxygen, or sulfur functionality. A detailed

(35) *Cambridge Structural Database System*; Cambridge Crystallographic Data Center: Cambridge, 1996.
(36) Chandrasekhar; V.; Chivers, T.; Parvez, M. *Acta Crystallogr., Sect. C* **1993**, *C49*, 393.
(37) Ahmed, F. R.; Pollard, D. R. *Acta Crystallogr.* **1971**, *B27*, 163.
(38) Ahmed, F. R.; Pollard, D. R. *Acta Crystallogr.* **1971**, *B27*, 172.
(39) Klement, U.; Schmidpeter, A. *Z. Naturforsch.* **1968**, *23b*, 1610.

**Table 1.** X-ray Crystallographic Parameters

(a) For **1**, **2**, **7**, **9**, and **10**

| Crystal data | **1** | **2** | **7** | **9** | **10** |
|---|---|---|---|---|---|
| empirical formula | $C_{14}H_{24}F_4N_5O_2P$ | $C_{18}H_{32}F_4N_5O_2P$ | $C_{13}H_{18}F_8N_4O_4P_2$ | $C_5H_{10}Cl_4N_4P_2$ | $C_7H_{14}Cl_4N_4P_2$ |
| formula wt | 401.35 | 457.46 | 508.25 | 329.91 | 357.96 |
| color | colorless | colorless | colorless | colorless | colorless |
| cryst size (mm) | 0.45 × 0.30 × 0.25 | 0.40 × 0.30 × 0.15 | 0.45 × 0.35 × 0.25 | 0.40 × 0.25 × 0.15 | 0.35 × 0.35 × 0.25 |
| cryst syst; space group | monoclinic; $P2_1/c$ | triclinic; $P\bar{1}$ | orthorhombic; $Cmc2_1$ | monoclinic; $P2_1/c$ | orthorhombic, $Fdd2$ |
| unit cell dimens | | | | | |
| $a$ (Å) | 12.0330(2) | 10.3677(1) | 20.9911(4) | 5.9212(1) | 32.2551(5) |
| $b$ (Å) | 15.7006(2) | 11.0883(3) | 10.9986(1) | 28.4835(1) | 32.5854(1) |
| $c$ (Å) | 10.0543(2) | 11.6401(3) | 8.6759(2) | 8.3399(2) | 5.8472(1) |
| α (deg) | | 102.140(2) | | | |
| $\beta$ (deg) | 99.887(1) | 96.234(2) | | 105.635(1) | |
| $\gamma$ (deg) | | 109.437(2) | | | |
| vol (Å$^3$) | 1871.36(5) | 1210.30(5) | 2003.03(6) | 1354.53(4) | 6145.67(14) |
| $Z$ | 4 | 2 | 4 | 4 | 16 |
| $\rho_{calc}$ (Mg/m$^3$) | 1.425 | 1.255 | 1.685 | 1.618 | 1.548 |
| $F(000)$ | 840 | 484 | 1032 | 664 | 2912 |
| absorption coeff (mm$^{-1}$) | 0.204 | 0.166 | 0.320 | 1.085 | 0.963 |
| temp (K) | 173(2) | 193(2) | 193(2) | 193(2) | 193(2) |
| $\theta$(max) (deg) | 27.72 | 24.68 | 27.02 | 24.61 | 27.16 |
| index ranges | $-13 \le h \le 15$ | $-12 \le h \le 10$ | $-23 \le h \le 26$ | $-6 \le h \le 6$ | $-40 \le h \le 39$ |
| | $-19 \le k \le 20$ | $-12 \le k \le 12$ | $-13 \le k \le 13$ | $-29 \le k \le 33$ | $-32 \le k \le 40$ |
| | $-13 \le l \le 12$ | $-11 \le l \le 13$ | $-10 \le l \le 10$ | $-9 \le l \le 5$ | $-7 \le l \le 7$ |
| no. of rflns collected | 9714 | 5565 | 4054 | 5930 | 7883 |
| no. of unique data | 3853 ($R_{int}$ = 0.0360) | 3797 ($R_{int}$ = 0.0330) | 1711 ($R_{int}$ = 0.0233) | 2228 ($R_{int}$ = 0.0581) | 2796 ($R_{int}$ = 0.0242) |
| $T$(max/min) ($\psi$-scan) | 0.905/0.833 | 0.987/0.856 | 0.954/0.732 | 0.983/0.535 | 0.967/0.897 |
| params refined | 332 | 399 | 170 | 176 | 187 |
| final indices (2$\sigma$ data), R1 (wR2) | 0.0466 (0.0949) | 0.0674 (0.1141) | 0.0384 (0.1032) | 0.0582 (0.1451) | 0.0208 (0.0516) |
| all data, R1 (wR2) | 0.0617 (0.1073) | 0.0981 (0.1284) | 0.0389 (0.1053) | 0.0651 (0.1555) | 0.0217 (0.0527) |
| goodness-of-fit, $S$ ($F^2$) | 1.129 | 1.210 | 1.111 | 1.178 | 1.060 |
| largest diff peak (e Å$^{-3}$) | 0.259 | 0.208 | 0.302 | 0.708 | 0.175 |
| largest diff hole (e Å$^{-3}$) | −0.297 | −0.252 | −0.469 | −0.565 | −0.162 |

(b) For 11, 12, 13, 14, 16

| crystal data | **11** | **12** | **13** | **14** | **16** |
|---|---|---|---|---|---|
| empirical formula | $C_{10}H_{21}ClN_5OP$ | $C_6H_4Cl_2F_4N_3O_2P$ | $C_7H_4Cl_2F_6N_3O_2P$ | $C_5H_4Cl_3N_3O_2P_2$ | $C_{18}H_{12}F_6N_3O_4P_2$ |
| formula wt | 293.74 | 327.99 | 378.00 | 382.40 | 479.28 |
| color | colorless | colorless | colorless | colorless | colorless |
| cryst size (mm) | 0.25 × 0.20 × 0.10 | 0.30 × 0.30 × 0.25 | 0.35 × 0.25 × 0.20 | 0.40 × 0.25 × 0.20 | 0.25 × 0.20 × 0.15 |
| cryst syst; space group | monoclinic; $C2/c$ | orthorhombic; $P2_12_12_1$ | monoclinic; $P2_1/c$ | orthorhombic; $P2_12_12_1$ | monoclinic; $P2_1/c$ |
| unit cell dimens | | | | | |
| $a$ (Å) | 23.0215(3) | 7.5910(3) | 10.1813(11) | 6.824(2) | 6.7885(4) |
| $b$ (Å) | 9.1538(2) | 12.4173(5) | 11.5192(12) | 10.423(3) | 14.7985(10) |
| $c$ (Å) | 15.0957(3) | 12.8871(4) | 10.9716(12) | 17.888(4) | 19.8511(13) |
| α (deg) | | | | | |
| $\beta$ (deg) | 109.964(1) | | 100.194(2) | | 94.108(1) |
| $\gamma$ (deg) | | | | | |
| vol (Å$^3$) | 2990.01(10) | 1214.73(8) | 1266.4(2) | 1272.2(5) | 1989.1(2) |
| $Z$ | 8 | 4 | 4 | 4 | 4 |
| $\rho_{calc}$ (Mg/m$^3$) | 1.305 | 1.793 | 1.983 | 1.997 | 1.600 |
| $F(000)$ | 1248 | 648 | 744 | 752 | 968 |
| abs coeff (mm$^{-1}$) | 0.360 | 0.714 | 0.721 | 1.020 | 0.226 |
| temp (K) | 193(2) | 293(2) | 173(2) | 193(2) | 193(2) |
| $\theta$(max) (deg) | 24.71 | 23.25 | 24.78 | 24.75 | 24.00 |
| index ranges | $-22 \le h \le 27$ | $-7 \le h \le 8$ | $-11 \le h \le 8$ | $-8 \le h \le 7$ | $-8 \le h \le 8$ |
| | $-10 \le k \le 10$ | $-13 \le k \le 9$ | $-13 \le k \le 7$ | $-3 \le k \le 12$ | $-18 \le k \le 18$ |
| | $-17 \le l \le 17$ | $-14 \le l \le 14$ | $-12 \le l \le 12$ | $-17 \le l \le 15$ | $-25 \le l \le 21$ |
| no. of rflns collected | 6507 | 4782 | 5627 | 2842 | 7896 |
| no. of unique data | 2520 ($R_{int}$ = 0.0333) | 1738 ($R_{int}$ = 0.0377) | 2134 ($R_{int}$ = 0.0213) | 1602 ($R_{int}$ = 0.0316) | 3099 ($R_{int}$ = 0.0486) |
| $T$(max/min) ($\psi$-scan) | 0.990/0.863 | 0.906/0.707 | 0.990/0.890 | 0.998/0.808 | 0.969/0.909 |
| params refined | 248 | 180 | 207 | 189 | 338 |
| final indices (2$\sigma$ data), R1 (wR2) | 0.0404 (0.0839) | 0.0257 (0.0666) | 0.0268 (0.0666) | 0.0356 (0.0773) | 0.0609 (0.1559) |
| all data, R1 (wR2) | 0.0510 (0.0898) | 0.0262 (0.0669) | 0.0290 (0.0682) | 0.0412 (0.0798) | 0.0921 (0.1657) |
| goodness-of-fit, $S$ ($F^2$) | 1.219 | 1.097 | 1.086 | 1.060 | 1.223 |
| largest diff peak (e Å$^{-3}$) | 0.257 | 0.335 | 0.394 | 0.242 | 0.303 |
| largest diff hole (e Å$^{-3}$) | −0.246 | −0.249 | −0.299 | −0.249 | −0.303 |

(c) For **17**−**19**, and **II**

| crystal data | **17** | **18** | **19** | **II** |
|---|---|---|---|---|
| empirical formula | $C_{18}H_{12}F_6N_3O_2PS_2$ | $C_{10}H_{16}F_4N_5O_2P$ | $C_{11}H_{16}F_6N_5O_2P$ | $C_5Cl_5N_3P_2$ |
| formula wt | 511.40 | 345.25 | 395.26 | 193.23 |
| color | pale yellow | colorless | colorless | colorless |
| cryst size (mm) | 0.40 × 0.20 × 0.10 | 0.35 × 0.15 × 0.15 | 0.50 × 0.25 × 0.25 | 0.45 × 0.25 × 0.20 |
| crystal syst; space group | rhombohedral; $R\bar{3}$ | monoclinic; $C2/c$ | orthorhombic; $Pbca$ | orthorhombic; $Pbca$ |

**Table 1** (Continued)

(c) For **17**−**19**, and **II**

| crystal data | **17** | **18** | **19** | **II** |
|---|---|---|---|---|
| unit cell dimen | | | | |
| *a* (Å) | 19.9027(3) | 11.1134(4) | 14.3554(2) | 16.8521(2) |
| *b* (Å) | | 28.5418(13) | 9.7834(1) | 7.8044(1) |
| *c* (Å) | | 10.5909(5) | 23.3805(3) | 29.4361(2) |
| α (deg) | 117.602(1) | | | |
| *β* (deg) | | 119.754(1) | | |
| *γ* (deg) | | | | |
| vol (Å$^3$) | 3124.36(8) | 2916.5(2) | 3283.67(7) | 3871.45(7) |
| *Z* | 6 | 8 | 8 | 16 |
| $\rho_{calc}$ (Mg/m$^3$) | 1.631 | 1.573 | 1.599 | 2.012 |
| *F*(000) | 1548 | 1424 | 1616 | 2272 |
| absorption coeff (mm$^{-1}$) | 0.407 | 0.248 | 0.248 | 1.769 |
| temp (K) | 193(2) | 173(2) | 193(2) | 193(2) |
| *θ*(max) (deg) | 23.00 | 23.26 | 27.08 | 25.00 |
| index ranges | $-19 \le h \le 20$ | $-12 \le h \le 8$ | $-13 \le h \le 18$ | $-17 \le h \le 20$ |
| | $1 \le k \le 20$ | $-25 \le k \le 31$ | $-12 \le k \le 12$ | $-9 \le k \le 9$ |
| | $-23 \le l \le 3$ | $-6 \le l \le 10$ | $-27 \le l \le 29$ | $-33 \le l \le 35$ |
| no. of rflns collected | 2909 | 2634 | 15656 | 15606 |
| no. of unique data | 2909 ($R_{int} = 0.0381$) | 1615 ($R_{int} = 0.0328$) | 3315 ($R_{int} = 0.0497$) | 3399 ($R_{int} = 0.0323$) |
| *T*(max/min) (*ψ*-scan) | 0.978/0.853 | 0.940/0.809 | 0.961/0.751 | 0.992/0.827 |
| params refined | 350 | 230 | 279 | 200 |
| final indices (2*σ* data), R1 (wR2) | 0.0583 (0.1099) | 0.0691 (0.1752) | 0.0472 (0.1221) | 0.0360 (0.0664) |
| all data, R1 (wR2) | 0.0723 (0.1242) | 0.0833 (0.1970) | 0.0576 (0.1295) | 0.0415 (0.0682) |
| goodness-of-fit, *S* (F$^2$) | 1.179 | 1.131 | 1.080 | 1.221 |
| largest diff peak (e Å$^{-3}$) | 0.252 | 0.380 | 0.372 | 0.280 |
| largest diff hole (e Å$^{-3}$) | −0.271 | −0.351 | −0.281 | -0.262 |

**Table 2.** Bond Lengths (Å) and Angles (deg) for **1**

| | | | |
|---|---|---|---|
| P(1)−N(1) | 1.585(2) | N(3)−C(10) | 1.352(3) |
| P(1)−N(3) | 1.586(2) | N(4)−C(5) | 1.352(3) |
| P(1)−O(1) | 1.592(2) | N(4)−C(6) | 1.468(3) |
| P(1)−O(2) | 1.603(2) | N(4)−C(8) | 1.473(3) |
| N(1)−C(5) | 1.358(3) | N(5)−C(10) | 1.358(3) |
| N(2)−C(10) | 1.360(3) | N(5)−C(11) | 1.469(3) |
| N(2)−C(5) | 1.362(3) | N(5)−C(13) | 1.472(3) |
| N(1)−P(1)−N(3) | 115.60(9) | C(10)−N(5)−C(13) | 120.0(2) |
| O(1)−P(1)−O(2) | 102.24(8) | C(11)−N(5)−C(13) | 117.3(2) |
| C(5)−N(1)−P(1) | 114.87(14) | N(4)−C(5)−N(1) | 116.7(2) |
| C(10)−N(2)−C(5) | 118.9(2) | N(4)−C(5)−N(2) | 115.7(2) |
| C(10)−N(3)−P(1) | 114.97(14) | N(1)−C(5)−N(2) | 127.6(2) |
| C(5)−N(4)−C(6) | 121.3(2) | N(3)−C(10)−N(5) | 116.4(2) |
| C(5)−N(4)−C(8) | 121.3(2) | N(3)−C(10)−N(2) | 127.7(2) |
| C(6)−N(4)−C(8) | 117.4(2) | N(5)−C(10)−N(2) | 115.9(2) |
| C(10)−N(5)−C(11) | 122.3(2) | | |

**Table 3.** Bond Lengths (Å) and Angles (deg) for **2**

| | | | |
|---|---|---|---|
| P(1)−N(1) | 1.579(3) | N(4)−C(5) | 1.355(5) |
| P(1)−N(3) | 1.583(3) | N(4)−C(6) | 1.447(6) |
| P(1)−O(1) | 1.598(2) | N(4)−C(9) | 1.471(5) |
| P(1)−O(2) | 1.603(2) | N(5)−C(12) | 1.353(5) |
| O(1)−C(1) | 1.436(4) | N(5)−C(16) | 1.465(5) |
| O(2)−C(4) | 1.430(4) | N(5)−C(13) | 1.467(5) |
| N(1)−C(5) | 1.361(4) | C(1)−C(2) | 1.503(5) |
| N(2)−C(5) | 1.346(5) | C(2)−C(3) | 1.531(5) |
| N(2)−C(12) | 1.351(4) | C(3)−C(4) | 1.503(5) |
| N(3)−C(12) | 1.364(4) | C(3)−C(4) | 1.503(5) |
| N(1)−P(1)−N(3) | 115.6(2) | C(12)−N(5)−C(13) | 121.6(4) |
| O(1)−P(1)−O(2) | 102.01(12) | C(16)−N(5)−C(13) | 116.6(4) |
| C(5)−N(1)−P(1) | 114.7(3) | N(2)−C(5)−N(4) | 116.0(3) |
| C(5)−N(2)−C(12) | 118.8(3) | N(2)−C(5)−N(1) | 128.0(3) |
| C(12)−N(3)−P(1) | 114.5(3) | N(4)−C(5)−N(1) | 116.0(4) |
| C(5)−N(4)−C(6) | 121.7(4) | N(2)−C(12)−N(5) | 115.9(3) |
| C(5)−N(4)−C(9) | 121.1(4) | N92)−C(12)−N(3) | 128.0(3) |
| C(6)−N(4)−C(9) | 117.1(4) | N(5)−C(12)−N(3) | 116.0(3) |
| C(12)−N(5)−C(16) | 121.6(3) | | |

investigation of both mono- and dicarbaphosphazenes with functionalities on the ring carbon atoms was, therefore, undertaken in this study.

The X-ray structures of **1**, **2**, and **7** confirm that the C−N bond in trialkylamines is activated, resulting in the substitution of the C−Cl bonds along with the formation of a seven-membered spirocycle at the phosphorus atom(s). Selected bond

**Table 4.** Bond Lengths (Å) and Angles (deg) for **7**[a]

| | | | |
|---|---|---|---|
| P(1)−N(1) | 1.572(3) | N(2)−P(1)$^{\dagger}$ | 1.584(2) |
| P(1)−N(2) | 1.584(2) | N(3)−C(1) | 1.330(5) |
| P(1)−O(2) | 1.594(2) | N(3)−C(6) | 1.477(3) |
| P(1)−O(1) | 1.596(2) | N(3)−C(6)$^{\dagger}$ | 1.478(3) |
| N(1)−C(1) | 1.365(3) | C(1)−N(1)$^{\dagger}$ | 1.365(3) |
| N(1)−P(1)−N(2) | 118.76(13) | C(1)−N(3)−C(6)$^{\dagger}$ | 121.1(2) |
| O(2)−P(1)−O(1) | 102.60(9) | C(6)−N(3)−C(6)$^{\dagger}$ | 117.4(3) |
| C(1)−N(1)−P(1) | 121.1(2) | N(3)−C(1)−N(1)$^{\dagger}$ | 117.3(2) |
| P(1)−N(2)−P(1)$^{\dagger}$ | 114.0(2) | N(3)−C(1)−N(1) | 117.3(2) |
| C(1)−N(3)−C(6) | 121.1(2) | N(1)$^{\dagger}$−C(1)−N(1) | 125.4(3) |

[a] Symmetry transformations used to generate equivalent atoms (†) $-x, y, z$.

**Table 5.** Bond Lengths (Å) and Angles (deg) for **9**

| | | | |
|---|---|---|---|
| Cl(1A)−P(1) | 2.012(2) | P(2)−N(3) | 1.598(3) |
| Cl(1B)−P(1) | 2.024(2) | P(2)−N(2) | 1.600(4) |
| Cl(2A)−P(2) | 2.029(2) | N(1)−C(1) | 1.364(6) |
| Cl(2B)−P(2) | 2.015(2) | N(3)−C(1) | 1.364(5) |
| P(1)−N(1) | 1.594(4) | N(4)−C(1) | 1.356(5) |
| P(1)−N(2) | 1.602(4) | N(4)−C(4) | 1.479(6) |
| | | N(4)−C(2) | 1.488(6) |
| N(1)−P(1)−N(2) | 118.6(2) | C(4)−N(4)−C(2) | 117.7(4) |
| N(3)−P(2)−N(2) | 118.9(2) | N(4)−C(1)−N(1) | 115.7(4) |
| C(1)−N(1)−P(1) | 120.6(3) | N(4)−C(1)−N(3) | 116.7(4) |
| P(2)−N(2)−P(1) | 113.8(2) | N(1)−C(1)−N(3) | 127.6(4) |
| C(1)−N(3)−P(2) | 120.0(3) | N(4)−C(2)−C(3) | 112.3(4) |
| C(1)−N(4)−C(4) | 121.4(4) | N(4)−C(4)−C(5) | 112.4(4) |
| C91)−N(4)−C(2) | 120.994) | | |

(40) Boldeskul, I. E.; Tarasevich, A. J.; Obodovskaya, A. E.; Starikova, Z. A.; Kornuta, P. P. *Zh. Obshch. Khim.* **1990**, *60*, 1975.
(41) Chernega, A. N.; Boldeskul, I. E.; Antipin, M. Yu.; Struchkov, Yu. I. *Zh. Strukt. Khim.* **1990**, *31*, 197.
(42) Meyer, M.; Klingebiel, U.; Kadel, J.; Oberhammer, H. *Z. Naturforsch.* **1988**, *43b*, 1010.
(43) Boldeskul, I. E.; Tarasevich, A. J.; Obodovskaya, A. E.; Struchkov, Yu. T; Kornuta, P. P.; Kolotilov, M. V. *Zh. Obshch. Khim.* **1987**, *57*, 1980.
(44) Chernega, A. N.; Antipin, M. Yu.; Struchkov, Yu. T.; Boldeskul, I. E. *Ukr. Khim. Zh.* **1993**, *59*, 306.

**Table 6.** Bond Lengths (Å) and Angles (deg) for **10**

| | | | |
|---|---|---|---|
| Cl(1A)−P(1) | 2.0112(8) | P(2)−N(2) | 1.591(2) |
| Cl(1B)−P(1) | 1.9967(8) | N(1)−C(1) | 1.358(2) |
| Cl(2A)−P(2) | 1.9979(7) | N(3)−C(1) | 1.356(2) |
| Cl(2B)−P(2) | 2.002(8) | N(4)−C(1) | 1.341(2) |
| P(1)−N(1) | 1.573(2) | N(4)−C(5) | 1.470(2) |
| P(1)−N(2) | 1.588(2) | N(4)−C(2) | 1.475(3) |
| P(1)−P(2) | 2.6611(7) | | |
| P(2)−N(3) | 1.573(2) | | |
| N(1)−P(1)−N(2) | 119.31(9) | C(1)−N(4)−C(2) | 121.4(2) |
| N(3)−P(2)−N(2) | 118.53(9) | C(5)−N(4)−C(2) | 117.4(2) |
| C(1)−N(1)−P(1) | 119.99(13) | N(4)−C(1)−N(3) | 116.6(2) |
| P(1)−N(2)−P(2) | 113.66(10) | N(4)−C(1)−N(1) | 116.1(2) |
| C(1)−N(3)−P(2) | 120.90(13) | N(3)−C(1)−N(1) | 127.3(2) |
| C(1)−N(4)−C(5) | 121.3(2) | | |

**Table 7.** Bond Lengths (Å) and Angles (deg) for **11**

| | | | |
|---|---|---|---|
| Cl(1)−P(1) | 2.0585(9) | N(4)−C(1) | 1.339(3) |
| P(1)−O(1) | 1.471(2) | N(4)−C(2) | 1.469(3) |
| P(1)−N(3) | 1.584(2) | N(4)−C(4) | 1.475(3) |
| P(1)−N(1) | 1.655(2) | N(5)−C(6) | 1.354(3) |
| N(1)−C(1) | 1.377(3) | N(5)−C(7) | 1.463(3) |
| N(2)−C(1) | 1.331(3) | N(5)−C(9) | 1.467(3) |
| N(2)−C(6) | 1.356(3) | C(2)−C(3) | 1.508(4) |
| N(3)−C(6) | 1.342(3) | | |
| O(1)−P(1)−N(3) | 118.90(10) | C(6)−N(5)−C(7) | 121.6(2) |
| O(1)−P(1)−N(1) | 113.16(9) | C(6)−N(5)−C(9) | 121.1(2) |
| N(3)−P(1)−N(1) | 106.62(10) | C(7)−N(5)−C(9) | 117.3(2) |
| C(1)−N(1)−P(1) | 121.0(2) | N(2)−C(1)−N(4) | 118.3(2) |
| C(1)−N(2)−C(6) | 120.1(2) | N(2)−C(1)−N(1) | 123.1(2) |
| C(6)−N(3)−P(1) | 119.4(2) | N(4)−C(1)−N(1) | 118.6(2) |
| C(1)−N(4)−C(2) | 123.5(2) | N(3)−C(6)−N(5) | 117.2(2) |
| C(1)−N(4)−C(4) | 118.9(2) | N(3)−C(6)−N(2) | 128.1(2) |
| C(2)−N(4)−C(4) | 117.3(2) | N(5)−C(6)−N(2) | 114.8(2) |

**Table 8.** Bond Lengths (Å) and Angles (deg) for **12**

| | | | |
|---|---|---|---|
| Cl(5)−C(5) | 1.742(3) | P(1)−N(3) | 1.598(3) |
| Cl(6)−C(6) | 1.731(3) | N(1)−C(5) | 1.299(3) |
| P(1)−O(1) | 1.558(2) | N(2)−C(5) | 1.326(4) |
| P(1)−O(2) | 1.562(2) | N(2)−C(6) | 1.333(3) |
| P(1)−N(1) | 1.595(2) | N(3)−C(6) | 1.304(3) |
| O(1)−P(1)−O(2) | 105.18(10) | C(6)−N(3)−P(1) | 114.7(2) |
| N(1)−P(1)−N(3) | 112.24(12) | N(1)−C(5)−N(2) | 131.7(2) |
| C(5)−N(1)−P(1) | 115.0(2) | N(3)−C(6)−N(2) | 131.4(2) |
| C(5)−N(2)−C(6) | 115.0(2) | | |

**Table 9.** Bond Lengths (Å) and Angles (deg) for **13**

| | | | |
|---|---|---|---|
| Cl(6)−C(6) | 1.746(2) | P(1)−N(3) | 1.611(2) |
| Cl(7)−C(7) | 1.729(2) | N(1)−C(7) | 1.305(3) |
| P(1)−O(1) | 1.5563(13) | N(2)−C(6) | 1.327(3) |
| P(1)−O(2) | 1.5605(13) | N(2)−C(7) | 1.344(3) |
| P(1)−N(1) | 1.609(2) | N(3)−C(6) | 1.307(3) |
| O(1)−P(1)−O(2) | 104.67(7) | C(6)−N(3)−P(1) | 115.28(14) |
| N(1)−P(1)−N(3) | 111.73(9) | N(3)−C(6)−N(2) | 131.5(2) |
| C(7)−N(1)−P(1) | 114.7(2) | N(1)−C(7)−N(2) | 131.8(2) |
| C(6)−N(2)−C(7) | 114.9(2) | | |

lengths and bond angles for amino-substituted spirocyclic carbaphosphazenes **1**, **2**, **7**, **18**, and **19** are listed in Tables 2−4, 13, and 14. The molecular structure of **1** (Figure 5) shows that the ethyl groups C6−C7 and C11−C12 lie above and C8−C9 and C13−C14 below, the $N_3PC_2$ core and are assigned as the up, down (*ud*) conformation. The torsion angles for the ethyl group arrangement are C5−N4−C6−C7 = −92.5(2)°, C5−N4−C8−C9 = −87.2(3)°, C10−N5−C11−C12 = −100.8(3)°, and C10−N5−C13−C14 = −88.4(2)°. The structure of **2**

(45) Obodovskaya, A. E.; Starikova, Z. A.; Boldeskul, I. E. *Dokl. Akad. Nauk Ukr. SSR, Ser. B* **1983**, *9*, 43.
(46) Chandrasekhar; V; Chivers, T.; Kumaravel, S. S.; Meetsma, A.; van de Grample, J. C. *Inorg. Chem.* **1991**, *30*, 3402.
(47) Hausen, H.-D.; Rajca, G.; Weidlein, J. *Z. Naturforsch., B* **1986**, *41B*, 839.

**Table 10.** Bond Lengths (Å) and Angles (deg) for **14**

| | | | |
|---|---|---|---|
| Cl(2A)−P(2) | 1.979(2) | P(1)−N(1) | 1.600(4) |
| Cl(2B)−P(2) | 1.983(2) | P(2)−N(2) | 1.561(4) |
| Cl(5)−C(5) | 1.748(5) | P(2)−N(3) | 1.609(4) |
| P(1)−O(2) | 1.567(3) | N(1)−C(5) | 1.334(7) |
| P(1)−O(1) | 1.577(4) | N(3)−C(5) | 1.303(7) |
| P(1)−N(2) | 1.584(4) | | |
| O(2)−P(1)−O(1) | 104.6(2) | C(5)−N(1)−P(1) | 117.3(4) |
| N(2)−P(1)−N(1) | 116.6(2) | P(2)−N(2)−P(1) | 116.3(3) |
| N(2)−P(2)−N(3) | 117.2(2) | N(3)−C(5)−N(1) | 133.3(5) |

**Table 11.** Bond Lengths (Å) and Angles (deg) for **16**

| | | | |
|---|---|---|---|
| P(1)−O(1) | 1.572(3) | O(4)−C(13) | 1.402(6) |
| P(1)−O(2) | 1.579(3) | N(1)−C(5) | 1.326(6) |
| P(1)−N(3) | 1.585(4) | N(2)−C(12) | 1.332(6) |
| P(1)−N(1) | 1.590(4) | N(2)−C(5) | 1.336(6) |
| O(1)−C(1) | 1.450(6) | N(3)−C(12) | 1.331(6) |
| O(2)−C(4) | 1.432(6) | C(1)−C(2) | 1.509(7) |
| O(3)−C(5) | 1.342(6) | C(2)−C(3) | 1.527(7) |
| O(3)−C(6) | 1.405(6) | C(3)−C(4) | 1.502(7) |
| O(4)−C(12) | 1.351(6) | | |
| O(1)−P(1)−O(2) | 104.1(2) | C(12)−N(2)−C(5) | 116.4(4) |
| N(3)−P(1)−N(1) | 114.2(2) | C(12)−N(3)−P(1) | 114.1(3) |
| C(5)−O(3)−C(6) | 119.7(4) | N(1)−C(5)−N(2) | 130.4(5) |
| C(12)−O(4)−C(13) | 119.4(4) | N(3)−C(12)−N(2) | 130.1(4) |
| C(5)−N(1)−P(1) | 114.0(3) | | |

**Table 12.** Bond Lengths (Å) and Angles (deg) for **17**

| | | | |
|---|---|---|---|
| S(2)−C(12) | 1.757(5) | N(3)−C(12) | 1.335(6) |
| S(2)−C(13) | 1.776(5) | C(5)−S(1A) | 1.775(10) |
| P(1)−O(1) | 1.563(3) | C(5)−S(1B) | 1.808(11) |
| P(1)−O(2) | 1.570(3) | C(6)−S(1A) | 1.733(12) |
| P(1)−N(3) | 1.591(4) | C(6)−S(1B) | 1.855(13) |
| P(1)−N(1) | 1.592(4) | C(9)−F(9B) | 1.41(3) |
| N(1)−C(5) | 1.322(6) | C(9)−F(9A) | 1.40(3) |
| N(2)−C(5) | 1.332(6) | C(16)−F(16B) | 1.362(6) |
| N(2)−C(12) | 1.338(6) | | |
| C(12)−S(2)−C(13) | 103.6(2) | N(2)−C(5)−S(1A) | 115.7(5) |
| O(1)−P(1)−O(2) | 104.6(2) | N(1)−C(5)−S(1B) | 109.1(6) |
| N(3)−P(1)−N(1) | 112.8(2) | N(2)−C(5)−S(1B) | 119.2(5) |
| C(5)−N(1)−P(1) | 115.1(3) | N(3)−C(12)−N(2) | 129.9(5) |
| C(5)−N(2)−C(12) | 115.9(4) | N(3)−C(12)−S(2) | 111.7(3) |
| C(12)−N(3)−P(1) | 115.3(3) | N(2)−C(12)−S(2) | 118.4(4) |
| N(1)−C(5)−N(2) | 130.9(4) | C(6)−S(1A)−C(5) | 107.1(6) |
| N(1)−C(5)−S(1A) | 112.8(5) | C(5)−S(1B)−C(6) | 100.8(6) |

(Figure 6) shows a disorder in one of the alkyl chains (C6−C8) which was modeled as a minor component (C7′ and C8′) and refined with an occupancy factor of 35%. The carbaphosphazene rings in **1** and **2** deviate from planarity with mean plane deviations of 0.023 Å [P1 = 0.033(1) and N3 = −0.032(1) Å] and 0.021 Å [P1 = 0.031(2) and N1 = −0.035 Å], respectively. The dispirocarbaphosphazene **7** crystallizes in a polar space group, $Cmc2_1$, and the absolute structure was determined reliably with Flack's parameter of 0.1(1). The molecule has a mirror plane containing the atoms C1, N2, and N3 (Figure 7a) which generates the other half of the molecule using the symmetry operation $-x, y, z$. The $N_3P_2C$ core is distorted, and C1 lies at 0.053 Å above the mean plane (deviation = 0.024 Å). Interestingly, the ethyl groups lie on the same side of the $N_3P_2C$ plane (*uu* conformation), which is different from the *ud* conformation of **1**. The torsion angles for the ethyl group are C1−N3−C6−C7 = 82.5(4)° and C1−N3−C6A−C7A = −82.5(4)°. This can be explained on the basis of the crystal packing for minimal steric repulsion between the two bulky spirocyclic fluoroalkoxy groups (Figure 7b). The molecular structure of the $N(CH_3)_2$-substituted dicarbaphosphazene **18** is shown in Figure 8a. The unit cell contains two crystallographically independent molecules. One of these molecules (molecule B) has a disorder in the seven-membered spirocyclic group. The two disordered spiro ring conformations (O2−C6−C7, F7A,

**Table 13.** Bond Lengths (Å) and Angles (deg) for **18**[a]

| | | | |
|---|---|---|---|
| P(1)−N(1) | 1.579(5) | N(3)−C(5) | 1.462(7) |
| P(1)−O(1) | 1.586(4) | N(4)−C(8) | 1.357(6) |
| P(2)−O(2) | 1.569(4) | N(5)−C(8) | 1.341(6) |
| P(2)−N(4) | 1.571(5) | N(6)−C(8) | 1.353(7) |
| O(1)−C(1) | 1.439(7) | N(6)−C(10) | 1.450(6) |
| O(2)−C(6′) | 1.25(2) | N(6)−C(9) | 1.454(7) |
| O(2)−C(6) | 1.32(2) | C(1)−C(2) | 1.503(8) |
| N(1)−C(3) | 1.355(7) | C(6)−C(7) | 1.443(13) |
| N(2)−C(3) | 1.347(6) | C(6′)−C(7) | 1.53(2) |
| N(3)−C(3) | 1.342(7) | C(7)−C(7)‡ | 1.508(14) |
| N(3)−C(4) | 1.455(8) | C(7)−C(7)‡ | 1.508(14) |

| | | | |
|---|---|---|---|
| N(1)−P(1)−N(1)† | 115.2(3) | C(8)‡−N(5)−C(8) | 119.0(6) |
| O(1)†−P(1)−O(1) | 101.5(3) | C(8)−N(6)−C(10) | 122.0(5) |
| O(2)−P(2)−O(2)‡ | 101.4(3) | C(8)−N(6)−C(9) | 122.7(4) |
| N(4)−P(2)−N(4)‡ | 114.8(3) | C(10)−N(6)−C(9) | 115.3(5) |
| C(3)−N(1)−P(1) | 115.4(4) | N(3)−C(3)−N(2) | 116.4(5) |
| C(3)†−N(2)−C(3) | 120.1(6) | N(3)−C(3)−N(1) | 116.6(5) |
| C(3)−N(3)−C(4) | 122.3(4) | N(2)−C(3)−N(1) | 127.0(5) |
| C(3)−N(3)−C(5) | 121.7(5) | N(5)−C(8)−N(6) | 116.3(4) |
| C(4)−N(3)−C(5) | 115.8(4) | N(5)−C(8)−N(4) | 127.6(5) |
| C(8)−N(4)−P(2) | 115.4(4) | N(6)−C(8)−N(4) | 116.1(5) |

[a] Symmetry transformations used to generate equivalent atoms: (†) $-x+1, y, -z+1/2$; (‡) $-x, y, -z+1/2$.

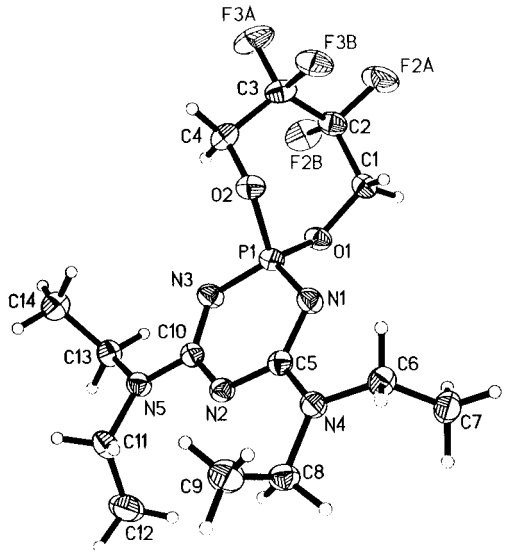


**Figure 5.** X-ray crystal structure of **1**.

**Table 14.** Bond Lengths (Å) and Angles (deg) for **19**

| | | | |
|---|---|---|---|
| P(1)−N(3) | 1.575(2) | N(3)−C(9) | 1.353(3) |
| P(1)−N(1) | 1.580(2) | N(4)−C(6) | 1.345(3) |
| P(1)−O(1) | 1.595(2) | N(4)−C(8) | 1.454(3) |
| P(1)−O(2) | 1.600(2) | N(4)−C(7) | 1.453(3) |
| N(1)−C(6) | 1.371(3) | N(5)−C(9) | 1.348(3) |
| N(2)−C(6) | 1.346(3) | N(5)−C(11) | 1.457(3) |
| N(2)−C(9) | 1.349(3) | N(5)−C(10) | 1.458(3) |

| | | | |
|---|---|---|---|
| N(3)−P(1)−N(1) | 116.62(10) | C(9)−N(5)−C(10) | 122.0(2) |
| C(6)−N(1)−P(1) | 113.9(2) | C(11)−N(5)−C(10) | 117.4(2) |
| C(6)−N(2)−C(9) | 119.6(2) | N(4)−C(6)−N(2) | 116.1(2) |
| C(9)−N(3)−P(1) | 114.3(2) | N(4)−C(6)−N(1) | 116.4(2) |
| C(6)−N(4)−C(8) | 122.0(2) | N(2)−C(6)−N(1) | 127.5(2) |
| C(6)−N(4)−C(7) | 122.8(2) | N(2)−C(9)−N(5) | 115.9(2) |
| C(8)−N(4)−C(7) | 115.2(2) | N92)−C(9)−N(3) | 128.0(2) |
| C(9)−N(5)−C(11) | 120.6(2) | N(5)−C(9)−N(3) | 116.1(2) |

F7B) and (O2−C6′−C7, F7A′, F7B′) were modeled with site occupancies of 63 and 37%, respectively (Figure 8b). The $N_3PC_2$ core is planar with atoms P1, P2, N2, and N5 lying on a 2-fold axis (Table 13). The complete molecular structures for A and B are generated by the symmetry operation $1-x, y, 1/2-z$ and $-x, y, 1/2+z$, respectively. The X-ray structural analysis of **19** (Figure 9) represents the first example of a phosphazene structure that contains an eight-membered spirocyclic group formed by a polyfluoroalkoxy group. The $N_3PC_2$ ring distorts slightly from planarity (mean plane deviation = 0.016 Å), and the eight-membered spiro ring adopts a pseudochair type of conformation with C1 and C5 deviating ~1.05 Å in the opposite direction from the $PO_2$ plane. The crystal packing shows parallel stacking of the $N_3P_2C$ rings along the *c*-axis with the spiro group lying normal to it. Selected bond lengths and angles for **II** are given in Table 15.

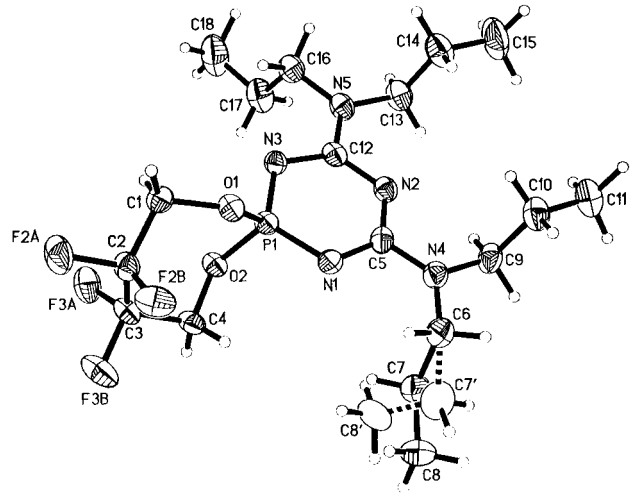


**Figure 6.** X-ray crystal structure of **2**.

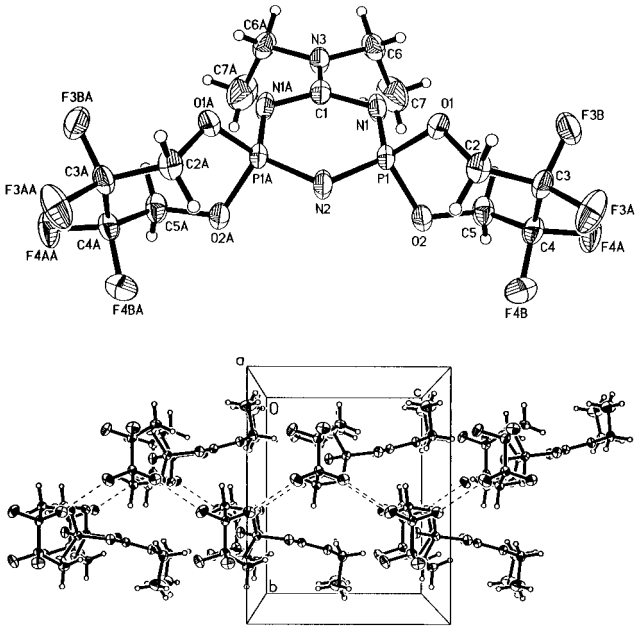


**Figure 7.** (a) X-ray crystal structure of **7**. (b) Crystal packing diagram for **7**: view along the *a*-axis.

In the dialkylamino-substituted dicarbaphosphazenes **1**, **2**, **18**, and **19**, the amino nitrogen atoms that form exocyclic C−N bonds are located in a planar environment, as suggested by the sum of angles ~360° around the exocyclic nitrogen atoms and their C−N−C−N torsion angles. For example, in **1** these torsion angles have values of −0.9(3) and −1.2(3)° for C6−N4−C5−N1 and C8−N4−C5−N2, and 10.0(3) and 2.8(3)° for C11−N5−C10−N2 and C13−N5−C10−N3, respectively. The seven-membered spirocyclic fluoroalkoxy group bonded to the phosphorus atom is puckered with C−F distances of ~1.36 Å. The P−O and P−N bond distances are ~1.59(1) and 1.580(5) Å while the O−P−O and N−P−N angles lie in the range 100.96(8)° for **19** to 102.24(4)° for **1** and at ~115.5°, respectively. The exocyclic C−N bond distances are ~1.351 Å and are almost similar to or slightly shorter than the endocyclic C−$N_P$ and C−$N_C$ distances 1.353(3)−1.371(3) ($N_P$, nitrogen

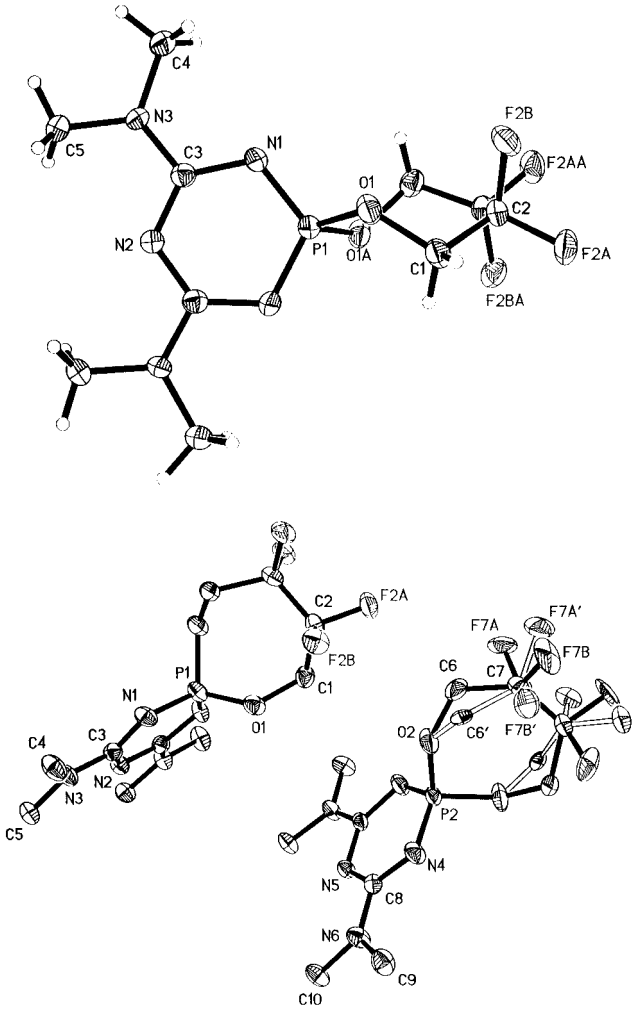


**Figure 8.** (a) X-ray crystal structure of **18**. (b) Disordered spiro rings in molecule B of **18**.

**Table 15.** Bond Lengths (Å) and Angles (deg) for **II**

| | | | |
|---|---|---|---|
| Cl(1)−P(1) | 1.9886(12) | Cl(6)−P(3) | 1.9881(12) |
| Cl(2)−P(1) | 1.9875(12) | Cl(7)−P(3) | 1.9840(12) |
| Cl(3)−P(2) | 1.9898(12) | Cl(8)−P(4) | 1.9883(12) |
| Cl(4)−P(2) | 1.9818(12) | Cl(9)−P(4) | 1.9871(12) |
| Cl(5)−C(1) | 1.753(3) | Cl(10)−C(2) | 1.756(3) |
| P(1)−N(1) | 1.587(3) | P(3)−N(4) | 1.587(3) |
| P(1)−N(3) | 1.606(3) | P(3)−N(6) | 1.613(3) |
| P(2)−N(1) | 1.589(3) | P(4)−N(4) | 1.583(3) |
| P(2)−N(2) | 1.608(3) | P(4)−N(5) | 1.611(3) |
| N(2)−C(1) | 1.327(4) | N(5)−C(2) | 1.321(4) |
| N(3)−C(1) | 1.320(4) | N(6)−C(2) | 1.321(4) |
| (N91)−P(1)−N(3) | 117.1(2) | N(4)−P(3)−N(6) | 116.62(14) |
| N(1)−P(2)−N(2) | 117.4(2) | N(4)−P(4)−N(5) | 117.02(14) |
| P(1)−N(1)−P(2) | 115.6(2) | P(4)−N(4)−P(3) | 116.4(2) |
| C(1)−N(2)−P(2) | 117.8(2) | C(2)−N(5)−P(4) | 118.1(2) |
| C(1)−N(3)−P(1) | 118.4(2) | C(2)−N(6)−P(3) | 118.2(2) |
| N(3)−C(1)−N(2) | 133.1(3) | N(6)−C(2)−N(5) | 133.2(3) |

bonded to phosphorus atom) and 1.346(3)−1.362(3) Å ($N_C$, nitrogen bonded to the carbon atom). This shortening effect is quite pronounced in **7**, where C−N(exo) and C−$N_P$ distances are 1.330(5) and 1.365(3) Å, respectively. The P−$N_C$ [1.572(3) Å] and P−$N_P$ [1.584(2) Å] also vary in a similar manner, and the difference between the C−N and P−N bonds causes the six-membered $N_3P_2C$ ring to distort from a regular hexagonal arrangement. The O−P−O angle is slightly greater [102.6(1)°] than found in the corresponding $N_3PC_2$ derivatives. Replacement of a carbon with a phosphorus atom in the $N_3PC_2$ heterocycle causes a compression of the N−C−N angles from ∼128° in dicarbaphosphazenes to 125.4(3)° in **7**, which is much smaller than the N−C−N angle of 133.1(3)° for $N_3P_2CCl_5$.[10,34]

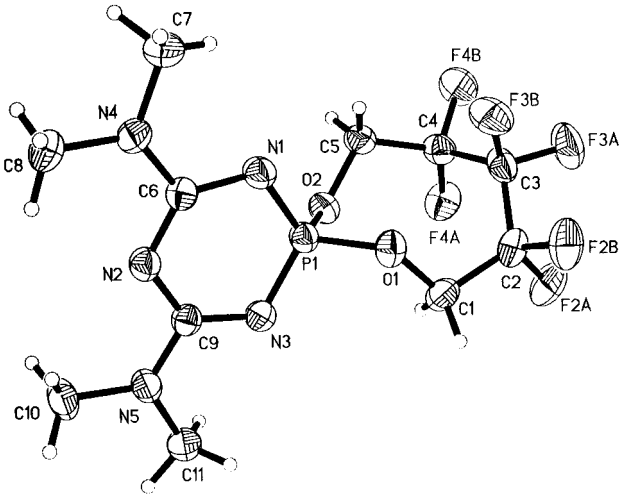


**Figure 9.** X-ray crystal structure of **19**.

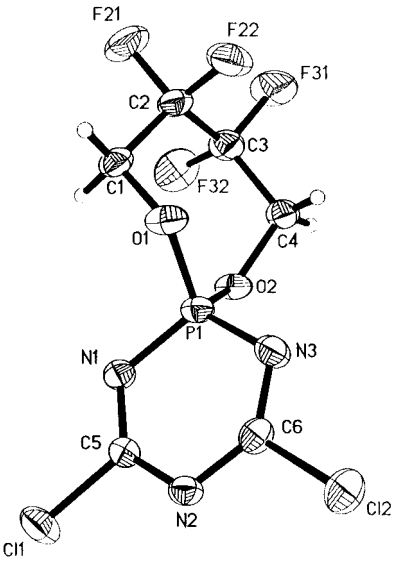


**Figure 10.** X-ray crystal structure of **12**.

Consequently, the C−N−P and N−P−N angles increase to 121.2(2) and 118.7(1)° from ∼116 and ∼115°, respectively, *vis-à-vis* dicarbaphosphazenes. The P−N−P angle of 114.0(2)° is much smaller than the corresponding angle in $N_3P_2C(OC_6H_5)_5$ [118.2(3)][10] and $N_3P_2CCl_5$ [∼116° (average)].[10,34]

The syntheses of the spirocyclic chlorodicarbaphosphazenes **12** and **13** provide an opportunity to carry out their structural analysis for comparison with their corresponding amino-substituted counterparts. Bond lengths and bond angles for these are listed in Tables 8 and 9. Compound **12** crystallizes in a non-centrosymmetric space group, $P2_12_12_1$, and its absolute configuration is determined reliably as the value of Flack's parameter is 0.00(8). The $N_3PC_2$ core is planar (mean plane deviation = 0.003 Å), with a puckered seven-membered spirocyclic fluoroalkoxy group lying perpendicular to it (Figure 10). The molecular structure of **13** (Figure 11) shows the eight-membered spiro group. The lopsided appearance of the spiro group results from the packing effects, where the molecules are inverted in a manner such that the spiro groups face away from each other. The presence of a chlorine atom on the carbaphosphazene ring carbon has some interesting effects. Compared to the corresponding features of the dialkylamino-substituted dicarbaphosphazene described above, the angles O−P−O and N−C−N and the P−N bond length increase to ∼105°, 131.5°, and ∼1.60 Å, respectively. Concurrently there is a contraction of the angles N−P−N = ∼112° and C−N−C = 115 °C. The C−$N_P$ and C−$N_C$ bond lengths are nonequiva-

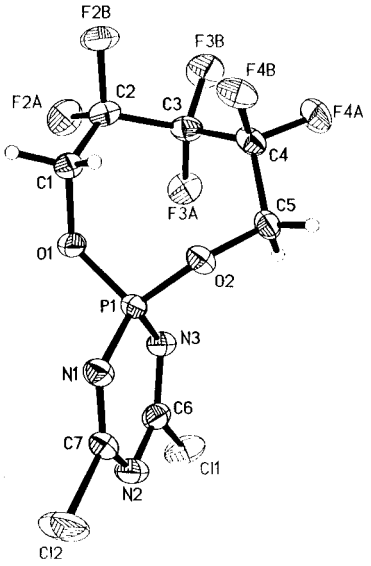


**Figure 11.** X-ray crystal structure of **13**.

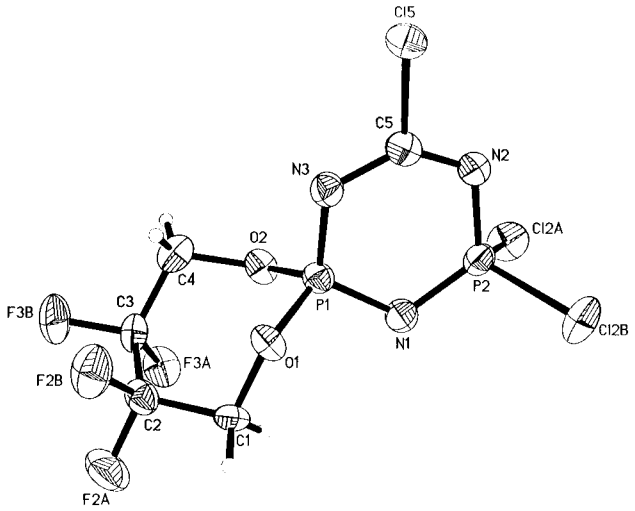


**Figure 12.** X-ray crystal structure of **14**.

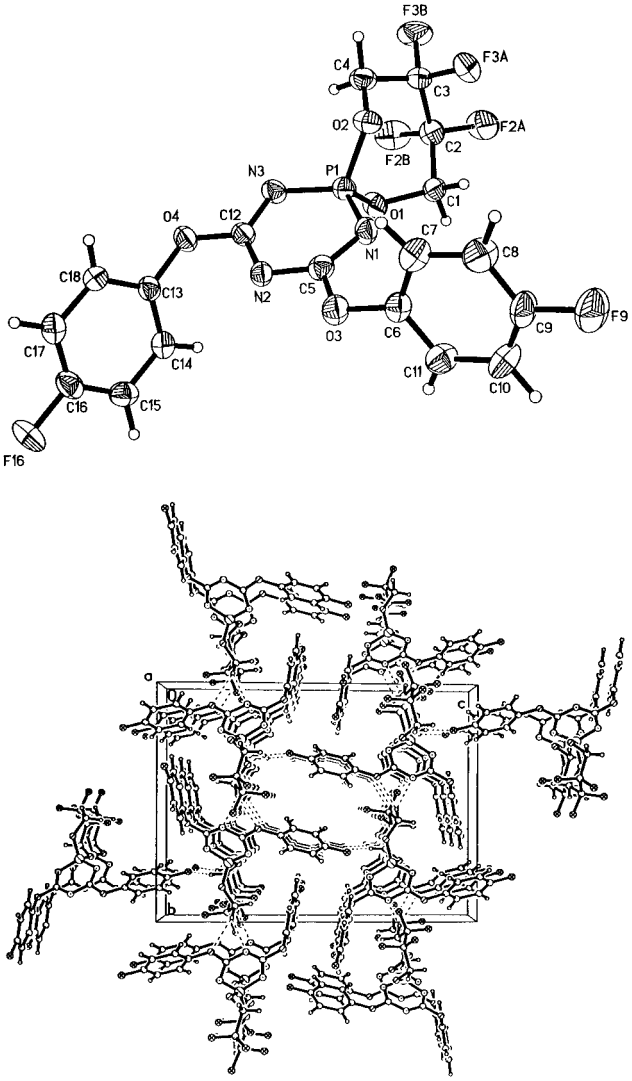


**Figure 13.** (a) X-ray crystal structure of **16**. (b) Crystal packing diagram for **16**: view along the *a*-axis.

lent, at 1.304 and 1.330 Å, respectively, and are considerably shorter than those of the amino derivatives.

An explanation for these structural differences may be based on the electronic nature of the substituent present on the carbon atom in the $N_3PC_2$ ring. In the case of amino-substituted carbaphosphazenes, the lone pair present on the exocyclic dialkylamino nitrogen atom causes mobilization of $\pi$-electron density toward the $N_3PC_2$ ring, thereby inducing a polarizing effect. With the availability of an enhanced electron density within the $N_3PC_2$ ring, there is an effective $p\pi-d\pi$ bonding between the nitrogen and phosphorus atoms, resulting in P−N bond shortening. In order to explain the short nature of the $C-N_P$ bond *versus* the $C-N_C$ bond, a canonical form comprising a $N_3PC_2$ ring with a negative charge on $N_C$ (located opposite to the phosphorus atom in the ring) and a positive charge on the phosphorus atom has been suggested.[40,41,43] In the case of $\sigma$-electron-withdrawing groups[43] like $CF_3$, $CCl_3$, or Cl, the involvement of the ring nitrogen lone pair is minimized, thereby resulting in the elongation of the P−N bond along with compression of the N−C−N angle.

The monospiro chlorocarbaphosphazene **14** crystallizes in an orthorhombic polar space group, $P2_12_12_1$. The Flack's parameter is refined to −0.05(13), which suggests that the atomic configuration assigned initially is correct. The $N_3P_2C$ core is puckered with P1, N1, N2, and N3 deviating significantly out of the mean plane by 0.0854, 0.517, 0.0552, and −0.0528 Å (Figure 12). The structural parameters listed in Table 10 are similar to those of $N_3P_2CCl_5$.[10,34] The N−P−N angles of 116.6(2)° and 117.2(2)° are much wider than in the dicarbaphosphazene analogue **12**, but smaller than the 119.1° (average) found in $N_3P_3F_4(OCH_2CF_2)_2$.[18] The crystal lattice shows an interaction arising from H1A···N3$^d$ at 2.579 Å (d = $^1/_2 + x$, $^3/_2 - y$, $-z$).

The *p*-fluorophenoxy-substituted carbaphosphazene **16** contains a distorted $N_3PC_2$ ring with the maximum deviation observed for P1 (−0.059 Å) and N3 (0.051 Å) (mean deviation = 0.039 Å). The two phenyl rings are twisted at 72.9(1)° and 73.4(1)° with respect to the $N_3PC_3$ ring and at 63.6(2)° with respect to each other (Figure 13a). The torsion angle values of C6−O3−C5−N1 [8.0(7)°] and C13−O4−C12-N3 [170.4(4)°] describe the orientation of these phenoxy rings with respect to the carbaphosphazene ring. The shortness of the C5−O3 [1.342(6) Å] and C12−O4 [1.352(6) Å] compared to the C6−O3 [1.405(6) Å] and C13−O4 [1.402(6) Å] bonds (Table 11) clearly demostrates the $\pi$-electron-donating ability of the *p*-fluorophenoxy substituent. In perfluorinated diphenyl ethers, bond distances of ∼1.38−1.39 Å are generally observed.[15] The packing diagram of **16** shows a H4B···F9$^a$ interaction of 2.456 Å (a = $1 + x$, $^3/_2 - y$, $^1/_2 + z$). In addition, there are two more long-range interactions: H1A···O3$^b$ = 2.436 Å (b = $1 - x$, $-^1/_2 + y$, $^1/_2 - z$) and H1A···N2$^b$ = 2.503 Å (Figure 13b). The participation of an alkyl proton in fluoroalkyl compounds in the formation of multicentered hydrogen bonding has recently

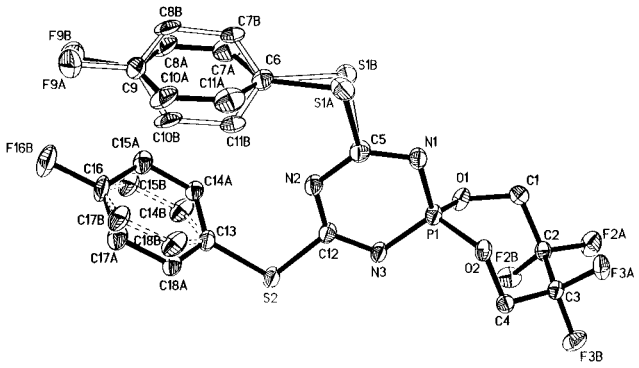


**Figure 14.** X-ray crystal structure of **17**.

been reported.[48] Compound **17** crystallized in a rhombohedral crystal system, and the structure was solved in the $R\bar{3}$ space group. The X-ray structure determination of **17** was complicated as the *p*-fluorothiophenoxy groups on both C5 and C12 show rotational as well as vibrational disorder (Figure 14). Interestingly, the orientation of the phenoxy groups is entirely different compared to that in **16**. The $N_3PC_2$ ring and rings C6−C11A and C13−C18A are twisted at 89.9(8) and 72.0(5)°, respectively. The phenyl rings are almost parallel and are twisted at 26° (component A) and 41.3(8)° (component B) with respect to each other. The disordered components in both the rings show a twist of ∼27°. The torsion angle values of C6−S1A−C5−N1 [173.3(6)°] and C13−S2−C12−N3 [175.0(4)°] show that the orientation of thiophenoxy rings with respect to the carbaphosphazene ring is very different from that found in **16**. The bond lengths and angles (Table 12) suggest that, for these derivatives, the O−P−O angles are closer to those of the chloro precursor. The C5−S2 distance [1.757(5) Å] is shorter than the C13−S2 distance [1.776(5) Å] as observed in the *p*-fluorophenoxy counterpart. For **16**, the N−P−N angle of 114.2(2)° is closer to the values observed for the amino derivatives whereas, for **17**, this value [112.8(2)°] resembles those found in **12** and **13**.

In compound **8**, the P−Cl bond is highly susceptible to hydrolysis. It has been proposed that these compounds exist as tautomers[28,32] where the P−OH proton resonates between the P═O and the α-nitrogen atom. Structural analysis of the hydrolyzed product **11** shows that only the chlorophosphoryl isomer is present, with the proton located on the nitrogen atom (Figure 15a). The final difference electron density map in the refinement does not show any residual electron density around the oxygen atom, thereby excluding the presence of a P−OH bond. Due to the protonation of the ring, the ring becomes high unsymmetrical, as seen from the structural parameters listed in Table 7. The $N_3PC_2$ core undergoes distortion with P1 and N1 out of the ring mean plane (mean deviation = 0.047 Å) by −0.088 and 0.061 Å. The P1−N3 bond length of 1.584(2) Å is much shorter than P1−N1 [1.655(2) Å], suggesting reduction to a single bond in the latter. The P−O bond at 1.471(2) Å also supports the formation of a P═O bond. The amino groups and the $N_3PC_2$ ring lie in the same plane, as shown by analysis of the planes described by C2−N4−C4 (2.2°) and C7−N5−C9 (5.2°). The conformation of the ethyl groups bonded to the nitrogen atoms is *uu* on N4 and *ud* on N5. The torsion angles for these groups at C1 and C6 are C3−C2−N4−C1 = −87.2(2)° and C5−C4−N4−C1 = 78.6(3)°, and C8−C7−N5−C6 = 89.1(3)° and C10−C9N5−C6 = 97.8(3)°. A unit cell packing diagram for **11** (Figure 15b) shows close intermolecular H1···O1$^c$ (c = $^1/_2 - x$, $^3/_2 - y$, $-z$) interactions at 2.031 Å with N1−H1···O1$^c$ = 162.8°. This results in the formation of dimers, which may be responsible for the unsymmetrical conformation of the ethyl groups.

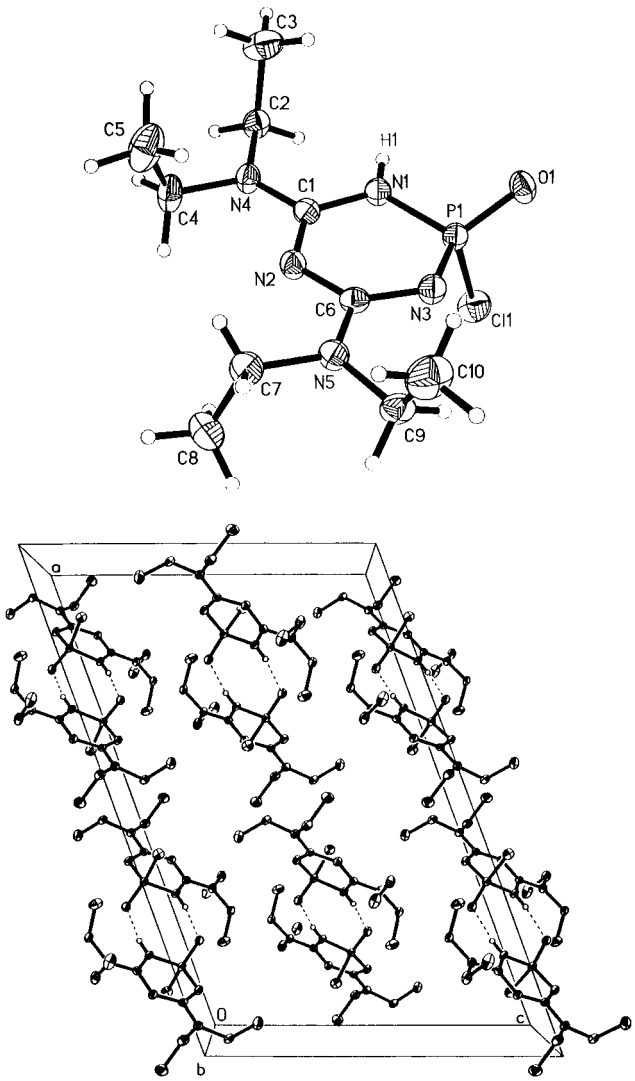


**Figure 15.** (a) X-ray crystal structure of **11**. (b) Unit packing diagram for **11**: view along the *b*-axis.

## Experimental Section

**Materials.** The reagents $NH_4Cl$, $PCl_5$, $Me_3SiN(CH_3)_2$, $N(C_2H_5)_3$, $N(C_3H_7)_3$, 1-methylpiperidine, 4-methylmorpholine, NaH, $CaH_2$, *n*-$C_4H_9$-Li, 4-$FC_6H_4OH$, and 4-$FC_6H_4SH$ (Aldrich) are used as received. Cyanamide (Aldrich) and $NaN(CN)_2$ (Fluka) are recrystallized from diethyl ether and stored under an inert atmosphere until ready for use. The polyfluoro diols $HOCH_2(CF_2)_nCH_2OH$ ($n$ = 2 or 3) (gift from 3M) are purified by vacuum sublimation twice before use. The cyclic chlorocarbaphosphazenes $N_3PC_2Cl_4$[28] and $N_3P_2CCl_5$[10] are prepared following a modified literature procedure and subsequently purified by sublimation and recystallization, respectively. The solvents diethyl ether, tetrahydrofuran, toluene, nitrobenzene, pentane, hexane, $CDCl_3$, chloroform, 1,2-dichloroethane, and 1,1,2,2-tetrachloroethane are dried prior to use by standard procedures and stored over molecular sieves (4 Å, Aldrich).

**General Procedures.** A conventional Pyrex glass vacuum line equipped with Heise Bourdon tube and Televac thermocouple gauges is used to transfer volatile materials using *PVT* techniques. Infrared spectra are recorded on a Perkin-Elmer 1710 FT-IR spectrophotometer as Nujol mulls between KBr disks. $^1$H, $^{13}$C, $^{19}$F, and $^{31}$P NMR spectra are obtained as $CDCl_3$ solutions on a Bruker AC300 FT-NMR spectrometer operating at 300.31 ($^1$H), 75.47 ($^{13}$C), 282.41 ($^{19}$F), and 121.92 ($^{31}$P) MHz, respectively. The $^1$H, $^{13}$C, $^{19}$F, and $^{31}$P chemical shifts are referenced to $(CH_3)_4Si$, $CDCl_3$, $CCl_3F$, and 85% $H_3PO_4$, respectively. Polymerization experiments involving $N_3P_2CCl_5$ and its derivatives are performed in 5 mm thick walled NMR tubes. A sealed

(48) Braden, D. A.; Gard, G. L.; Weakley, T. J. R. *Inorg. Chem.* **1996**, *35*, 1912 and references therein.

capillary containing DMSO-$d_6$ is inserted into the NMR tube that contains the neat solid sample (0.3−0.5 g). The NMR tube is then inserted into the probe which is preheated at 120 °C and tuned for $^{31}$P (121.92 MHz). After a minute for equilibration and a quick shim process lasting less than 5 min, the first dataset is recorded (assigned time = 0). FID data are then acquired at 10 min intervals for the first 2 h, 20 min intervals for the next 3 h, and then 1 h intervals, over a total period of 24 h. EI/CI mass spectra are obtained on a Varian VG 7070 HS mass spectrometer. Elemental analyses were performed by Beller Mikroanalytisches Laboratorium, Göttingen, Germany. Melting points (uncorrected) were obtained by using a Mel-Temp II apparatus. Manipulations and measurements were performed under inert atmospheric conditions.

**X-ray Diffraction Studies.** The X-ray diffraction data for compounds **1**, **2**, **7**, **9**−**14**, and **17**−**19** were collected on a Siemens SMART diffractometer with a CCD detector at −54 °C. Data collection parameters are listed in Table 1a,b. The frame data are acquired with the SMART[49] software using a Siemens three-circle platform using Mo K$_\alpha$ radiation ($\lambda$ = 0.710 73 Å) from a fine-focus tube. The $\chi$-axis on this platform is fixed at 54.74°, and the diffractometer is equipped with a CCD detector maintained near −54 °C. Cell constants are determined from 60 10 s frames. A complete hemisphere of data is scanned on $\omega$ (0.3°) with a run time of 10 s per frame at the detector resolution of 512 × 512 pixels. A total of 1271 frames are collected in three sets, and a final set of 50 frames, identical to first 50 frames, are also collected to determine crystal decay. The frames are then processed on a SGI-Indy/Indigo 2 workstation by using the SAINT software,[50] to give the *hkl* file corrected for Lp/decay. The structures are solved by the direct method using the SHELX-90[51] program and refined by a least squares method on $F^2$, SHELXL-93,[52] incorporated in SHELXTL-PC V 5.03.[53] In the case of **19**, the structure was initially solved in the nonstandard space group *I*2/*a* with *a* = 10.713(4) Å, *b* = 28.673(10) Å, *c* = 10.964(3)Å, $\beta$ = 117.27(0)°. Unit cell transformation to the standard *C*2/*c* gives new constants, listed in Table 1c. All non-hydrogen atoms are refined anisotropically. The hydrogen atoms are located from the difference electron density maps and are included in the refinement process in an isotropic manner. The hydrogen atoms on the following carbon atoms were added by the Riding model: **7**, C7; **10**, C4 and C7; **19**, C11. However, a riding model is used to include the hydrogen atoms in the disordered structures of **2**, **17**, and **18** (hydrogen atoms on the spiro group are located from difference electron density maps). All the crystals used for the diffraction studies showed no decomposition during data collection.

**Reaction of $N_3PC_2Cl_4$ (I) with $[CF_2CH_2OH]_2$ (III) and $N(C_2H_5)_3$.** $N_3PC_2Cl_4$ (1.36 g, 5.71 mmol) is placed in a round-bottomed flask fitted with a reflux condenser under an atmosphere of nitrogen. Toluene (25 mL) is transferred to the flask and the mixture stirred until a clear solution is obtained. $[CF_2CH_2OH]_2$ (0.93 g, 5.74 mmol) is added and the mixture stirred at 25 °C for 30 min. Triethylamine (3.45 g, 34.15 mmol) is added to this solution with stirring over a period of 15−30 min, during which the solution turns pale yellow with the formation of a viscous semisolid mass. On slow heating of the mixture to gentle reflux (bath temperature 125 °C), the semisolid dissolves and formation of another dark yellow solid is observed. After refluxing for 18−24 h, the mixture is cooled to 25 °C and volatile materials are removed *in vacuo* to yield a semisolid along with a crystalline mass. On extraction of this semisolid with hexane (2 × 10 mL), the crystalline part dissolves. When this solution is held at 0 °C for 12 h, white crystals are formed, which are characterized as $[CF_2CH_2O]_2PN_3C_2[N(C_2H_5)_2]_2$ (**1**) (0.76 g, 33%).

**Properties of $[CF_2CH_2O]_2PN_3C_2[N(C_2H_5)_2]_2$ (1).** Compound **1** is obtained as a colorless crystalline material (mp 71 °C). The spectral data for **1** are as follows. IR (cm$^{-1}$): 1544 s, 1500 s, 1462 s, 1430 s, 1402 s, 1360 s, 1347 s, 1317 s, 1303 s, 1285 m, 1238 m, 1141 s, 1111 s, 1094 s,1077 s, 1063 s, 1017 s, 972 w, 931 m, 921 m, 897 m, 823 m, 802 w, 786 w, 767 w, 708 w, 669 m, 606 w. NMR: $^1$H, $\delta$ 1.13 (t, 12H, $CH_3$), 3.48 (q, 8H, $NCH_2$, $^3J_{H-H}$ = 7.4 Hz), 4.38 (m, 4H, $OCH_2$); $^{19}$F, $\delta$ −127.63 (s, $CF_2$); $^{31}$P, $\delta$ 40.03 (pentet, $^3J_{P-H}$ = 16.1 Hz); $^{13}$C, $\delta$ 13.43 ($CH_3$), 40.91, 41.49 ($NCH_2$), 60.89 (m, $CH_2$), 113.12 (tt, $CF_2$, $^1J_{C-F}$ = 255 Hz, $^2J_{C-F}$ = 28 Hz), 164.7 (d, NCN, $^2J_{C-P}$ = 11.3 Hz). MS (EI) [*m/e* (species) intensity]: 401 ($M^+$) 50; 386 ($M^+$ − Me) 15; 372 ($M^+$ − Et) 100; 358 ($M^+$ + 1 − Me − Et) 35; 330 ($M^+$ − $NEt_2$ + 1) 20; 329 ($M^+$ − $NEt_2$) 19. Anal. Calcd for $C_{14}H_{24}F_4N_5O_2P$: C, 41.90; H, 5.99; N, 17.46. Found: C, 41.87; H, 5.93; N, 17.41.

The hexane portion of the extract after removal of **1** on evaporation *in vacuo* yielded a polymeric mass (0.50 g), which was found to contain $Cl_2PN_3C_2[N(C_2H_5)_2]_2$ [$^{31}$P, $\delta$ 56.20 ppm; $^{13}$C, $\delta$ 163.10[9] (d, NCN, $^2J_{C-P}$ = 8.5 Hz)] along with traces of **1**.[22]

**Reaction of $N_3PC_2Cl_4$ with $[CF_2CH_2OH]_2$ and $N(n\text{-}C_3H_7)_3$.** On reaction of 0.92 g (3.85 mmol) of $N_3PC_2Cl_4$ with $[CF_2CH_2OH]_2$ (0.62 g, 3.83 mmol) in the presence of tripropylamine (2.76 g, 27.25 mmol) in refluxing toluene under conditions identical with those described for the reaction with triethylamine, dark yellow solution is obtained. When the mixture is cooled at 4 °C for 2 h, fine crystals of tripropylamine hydrochloride along with a viscous oil form. The mixture is separated and the filtrate concentrated *in vacuo* to yield a dark yellow, viscous oil, which is extracted with hexane (2 × 10 mL). The hexane extract on cooling at 4 °C for 24 h gives $[CF_2CH_2O]_2PN_3C_2[N(n\text{-}C_3H_7)_2]_2$ (**2**) (0.65 g, 36%).

**Properties of $[CF_2CH_2O]_2PN_3C_2[N(n\text{-}C_3H_7)_2]_2$ (2).** Compound **2** is obtained as colorless crystalline blocks (mp 102 °C). The spectral data obtained for **2** are as follows. IR (cm$^{-1}$): 1543 s, 1489 vs, 1466 vs, 1430 s, 1413 s, 1379 s, 1363 s, 1321 m, 1287 m, 1276 m, 1239 m, 1217 w, 1180 w, 1142 s, 1113 s, 1093 s, 1036 m, 1006 m, 978 m, 924 m, 894 w, 871 vw, 825 m, 792 w, 767 vw, 746 vw, 711 vw, 669 m, 649 vw. NMR: $^1$H, $\delta$ 0.88 (m, 12H, $CH_3$), 1.57 (m, 8H, $CH_2$), 3.38 (q, 8H, $NCH_2$), 4.37 (m, 4H, $OCH_2$); $^{19}$F, $\delta$ −127.6 (s, $CF_2$); $^{31}$P, $\delta$ 39.92 (pentet, $^3J_{P-H}$ = 16.3 Hz); $^{13}$C, $\delta$ 11.52 ($CH_3$), 21.38 ($CH_2$), 49.39, 48.57 ($NCH_2$), 60.8 (m, $CH_2$), 113.2 (tt, $CF_2$, $^1J_{C-F}$ = 255 Hz, $^2J_{C-F}$ = 28 Hz), 165.17 (d, NCN, $^2J_{C-P}$ = 11.3 Hz). MS (EI) [*m/e*, (species), intensity]: 457 ($M^+$) 50; 442 ($M^+$ − Me) 35; 428 ($M^+$ − Et) 69; 414 ($M^+$ − Pr) 100.

Anal. Calcd for $C_{18}H_{32}N_5O_2F_4P$: C, 47.27; H, 7.00, N, 15.32. Found: C, 47.71; H, 7.02; N, 15.33

On complete removal of the solvent from the remaining hexane extract, a semisolid is obtained (0.40 g), which shows the presence of $Cl_2PN_3C_2[N(n\text{-}C_3H_7)_2]_2$ [$^{31}$P, $\delta$ 56.02 ppm; $^{13}$C, $\delta$ 164.8 (d, NCN, $^2J_{C-P}$ = 8.4 Hz)] as well as traces of **2**.

**Reaction of $N_3PC_2Cl_4$ with $[CF_2CH_2OH]_2$ and 1-methylpiperidine.** The reaction of 0.55 g (2.30 mmol) of $N_3PC_2Cl_4$ and $[CF_2CH_2OH]_2$ (0.37 g, 2.28 mmol) with 0.91 g (9.17 mmol) of -methylpiperidine, when carried out under conditions identical with those described for the reaction with triethylamine, is found to yield $[CF_2CH_2O]_2PN_3C_2[NCH_2(CH_2)_3CH_2]_2$ (**3**) and $Cl_2PN_3C_2[NCH_2(CH_2)_3CH_2]_2$ (**4**) as a mixture, which can be easily identified on the basis of $^{31}$P NMR chemical shifts. The NMR spectral data for this mixture is as follows: $^1$H, $\delta$ 1.40−1.60 [m, $(CH_2)_3$], 3.65 (m, $NCH_2$), 4.32 (m, $CH_2$); $^{19}$F, $\delta$ −127.6 (s, $CF_2$); $^{31}$P, $\delta$ 40.77 (pentet, $P_{spiro}$, $^3J_{P-H}$ = 16.2 Hz); 57.5 (s, $P_{PCl2}$); $^{13}$C, $\delta$ 24.91 ($CH_2$), 25.86 ($CH_2$), 44.43, 44.69 ($NCH_2$), 61.07 (m, $CH_2$), 113.09 (tt, $CF_2$, $^1J_{C-F}$ = 254 Hz, $^2J_{C-F}$ = 28 Hz), 163.2 [d, NCN(**4**), $^2J_{C-P}$ = 8.6 Hz], 164.9 [d, NCN(**3**), $^2J_{C-P}$ = 11.6 Hz]. MS (EI) [*m/e*, (species), intensity]: **3**, 425 ($M^+$) 7; 341 [$M^+$ − $NCH_2(CH_2)_4$] 5; 264 [$M^+$ − 1 −$(OCH_2CF_2)_2$] 38; **4**, 335 ($M^+$) 100; 300 ($M^+$ −Cl) 55; 252 [$M^+$ + 1 −$NCH_2(CH_2)_4$] 31.

**Reaction of $N_3PC_2Cl_4$ with $[CF_2CH_2OH]_2$ and 4-Methylmorpholine.** $N_3PC_2Cl_4$ (0.68 g, 2.85 mmol) and $[CF_2CH_2OH]_2$ (0.46 g, 2.84 mmol) are stirred in toluene (25 mL) at 50 °C for 2 h. The solution turns cloudy and is treated at 25 °C with 4-methylmorpholine (1.42 g, 14.04 mmol) over a period of 5 min. The solution, which initially gives a pale yellow flocculent precipitate, on heating slowly to 120 °C gives a dark yellow solution and a brown semisolid. After refluxing for 24 h the mixture is worked up similarly to that for the reaction with triethylamine. The solid compound obtained from the hexane extract is found to be a mixture of $[CF_2CH_2O]_2PN_3C_2[N(CH_2)_2O(CH_2)_2]_2$ (**5**) and $Cl_2PN_3C_2[N(CH_2)_2O(CH_2)_2]_2$ (**6**). NMR: $^1$H, $\delta$ 4.32 (m, $CH_2$), 3.60−3.67 (m, $NCH_2$ and $OCH_2$); $^{19}$F, $\delta$ −127.67 (s, $CF_2$); $^{31}$P, $\delta$ 40.1

(49) *SMART V 4.043 Software for the CCD Detector System*; Siemens Analytical Instruments Division: Madison, WI, 1995.
(50) *SAINT V 4.035 Software for the CCD Detector System*; Siemens Analytical Instruments Division, Madison, WI, 1995.
(51) Sheldrick, G. M. *SHELXS-90, Program for the Solution of Crystal Structure*; University of Göttingen: Göttingen, Germany, 1990.
(52) Sheldrick, G. M. *SHELXL-93, Program for the Refinement of Crystal Structure*; University of Göttingen: Göttingen Germany, 1993.
(53) *SHELXTL 5.03 (PC-Version), Program library for Structure Solution and Molecular Graphics*; Siemens Analytical Instruments Division: Madison, WI, 1995.

(pentet, $P_{spiro}$, $^3J_{P-H}$ = 16.3 Hz; 57.5 (s, $P_{PCl2}$); $^{13}$C, $\delta$ 43.74, 44.09 ($NCH_2$), 61.45 (m,$CH_2$), 66.75 ($OCH_2$), 112.95 (tt, $CF_2$, $^1J_{C-F}$ = 255 Hz, $^2J_{C-F}$ = 28 Hz), 163.6 [d, NCN(**6**), $^2J_{C-P}$ = 8.5 Hz], 165.3 [d, NCN(**5**), $^2J_{C-P}$ = 11.6 Hz]. MS (EI): **5**, [*m/e*, (species), intensity] 429 ($M^+$) 77; **6**, 339 ($M^+$); 304 ($M^+ - Cl$); 253 [$M^+ - N(CH_2)_2O(CH_2)_2$].

**Reaction of $N_3P_2CCl_5$ with $[CF_2CH_2OH]_2$ and $N(C_2H_5)_3$.** To a solution of $N_3P_2CCl_5$ (0.65 g, 2.22 mmol) in ~15 mL of toluene is added $[CF_2CH_2OH]_2$ (0.73 g, 4.52 mmol) in 5 mL of the same solvent. An excess of triethylamine (8 mmol) is added to the reaction mixture, and the contents are allowed to reflux for 16 h under a nitrogen atmosphere. Upon cooling to 25 °C, the reaction mixture is filtered and the solvent removed using a rotary evaporator. The beige residue is extracted with 2 × 5 mL portions of cold hexane. The residue is then sublimed at 120−130 °C/0.05 Torr, leaving a polymeric mass. The sublimate contains the dispiro derivative, $[(CF_2CH_2O)_2]_2P_2N_3CN(C_2H_5)_2$ (**7**), and triethylammonium hydrochloride salt, which is characterized from $^{13}$C NMR [$^{13}$C, $\delta$ 45.91 ($NCH_2$), 8.66 ($CH_3$) (lit. 46.05, 8.78)[54]]. Compound **7** can be easily purified by repeated extractions of the mixture with hexane.

**Properties of $[(CF_2CH_2O)_2]_2P_2N_3C[N(C_2H_5)_2]$ (7).** Compound **7** is isolated as a white microcrystalline material (mp 155−157 °C) in 37% yield. Crystals suitable for X-ray diffraction are grown from a mixture of chloroform and cyclohexane at 25 °C. The spectral data for this compound are as follows. IR ($cm^{-1}$): 1525 s, 1461 vs, 1439 vs, 1427 s, 1371 s, 1329 s, 1285 w, 1273 w, 1255 mw, 1235 m, 1177 vw, 1144 vs, 1136 vs, 1101 m, 1055 vs, 1010 m, 960 m, 934 w, 919 mw, 893 w, 836 m, 819 w, 781 mw, 762 w, 741 vw, 710 w, 671 ms. NMR: $^1$H, $\delta$ 1.37 (t, 6H,$CH_3$), 3.47 (q, 4H, $NCH_2$), 4.32 (m, 8H, $OCH_2$); $^{19}$F, $\delta$ −127.7 (s, $CF_2$); $^{31}$P, $\delta$ 28.4 (pentet, $^3J_{P-H}$ = 8.5 Hz); $^{13}$C, $\delta$ 13.2 (s, $CH_3$), 41.6 (s, $NCH_2$), 61.3 (m,$CH_2$), 112.8 (tt, $CF_2$, $^1J_{C-F}$ = 257 Hz, $^2J_{C-F}$ = 28 Hz,), 162.7 (t, NCN, $^2J_{C-P}$ = 17.7 Hz). MS (EI) [*m/e*, (species), intensity]: 508 ($M^+$) 29; 492 ($M^+ - CH_3$) 12; 479 ($M^+ - C_2H_5$) 49; 436 [$M^+ - N(C_2H_5)_2$] 100.

**Reaction of $N_3PC_2Cl_4$ with Excess $N(C_2H_5)_3$.** To a solution of $N_3PC_2Cl_4$ (0. 84 g, 3.53 mmol) in 25 mL of toluene is introduced triethylamine (2.86 g, 28.3 mmol) by syringe over a period of 5 min at 25 °C. A white precipitate forms gradually and remains as a pale yellow flocculent precipitate over a period of 1 h. The solution is warmed slowly to 120 °C in an oil bath. At 100 °C, all of the material is dissolved or suspended to give a turbid yellow solution. Refluxing is continued for a period of 18 h, and then the mixture is cooled to 25 °C under nitrogen. A white solid precipitates (0.22 g) and is characterized as triethylammonium hydrochloride by $^{13}$C NMR spectroscopy as described above. The filtrate is concentrated *in vacuo*, and all volatile materials are removed. The semicrystalline residue is extracted with hexane (5 × 3 mL), producing a pale yellow solution and a hexane-insoluble brown semisolid. The hexane extract on cooling at 0 °C forms crystalline $Cl_2PN_3C_2[N(C_2H_5)_2]_2$[22] (**8**) (0.90 g, 82%). NMR: $^1$H, $\delta$ 1.06 (t, 12H, $CH_3$), 3.40 (q, 8H, $NCH_2$) (lit. 1.18, 3.56);[22] $^{31}$P, $\delta$ 56.19 (s) (lit. 55.40);[22] $^{13}$C, $\delta$ 13.42 ($CH_3$), 41.36, 41.81 ($NCH_2$), 163.1 (d, NCN, $^2J_{C-P}$ = 8.1 Hz).

**Reactions of $N_3P_2CCl_5$ with $R_3N$ (R = $C_2H_5$ or *n*-$C_3H_7$).** To a solution of $N_3P_2CCl_5$ (2.95 g, ~10.1 mmol) in toluene at 25 °C is added ~25 mmol of triethylamine or tri-*n*-propylamine. The reaction mixture is then refluxed for 12 h under nitrogen, after which all the volatile materials are removed under vacuum. The residue is extracted three times with hexane and filtered to remove any insoluble material. Removal of the solvent using a rotary evaporator affords an off-white solid, which is subsequently sublimed twice at 0.03 Torr at 110−120 °C to yield a white solid in 80−85% yield, characterized as the dialkylamino-substituted monocarbaphosphazene.

**Properties of $Cl_4P_2N_3CN(C_2H_5)_2$ (9).** $Cl_4P_2N_3CN(C_2H_5)_2$ is a white solid and has been obtained *via* a different route earlier.[22] Spectral data, not reported earlier for this compound, are as follows. IR ($cm^{-1}$): 1580 vs, 1540 vs, 1461 vs, 1440 vs, 1395 vs, 1349 ms, 1319 vs, 1251 vs, 1231 s, 1193 ms, 1170 ms, 1143 ms, 1121 s, 1078 s, 1005 s, 951 w, 908 s, 848 vw, 830 vw, 797 m, 779 m, 731 m, 646 ms, 623 ms. NMR: $^1$H, $\delta$ 1.18 (t, 3H, $CH_3$), 3.48 (q, 2H, $CH_2$); $^{31}$P, $\delta$ 36.1 (s); $^{13}$C, $\delta$ 13.4 ($CH_3$), 42.3 ($CH_2$), 159.5 (t, NCN, $^2J_{C-P}$ = 10.3 Hz). MS (EI) [*m/e*, (species), intensity]: 330 ($M^+$) 75; 315 ($M^+ - CH_3$) 100; 301 ($M^+ - C_2H_5$) 46; 295 ($M^+ - Cl$) 65; 258 [$M^+ - N(C_2H_5)_2$] 98.

**Properties of $Cl_4P_2N_3C[N(C_3H_7)_2]$ (10).** $Cl_4P_2N_3C[N(C_3H_7)_2]$ is isolated as a white solid (mp 78−79 °C). The spectral data obtained for this compound are as follows. IR ($cm^1$): 1587 w, 1527 vs, 1464 s, 1397 vs, 1378 vs, 1324 s, 1283 s, 1229 ms, 1206 sh, 1147 m, 1124 s, 1033 m, 997 ms, 957 s, 892 m, 881 m, 794 mw, 730 ms, 672 s. NMR: $^1$H, $\delta$ 0.89 (t, 3H, $CH_3$), 1.60 (sextet, 2H, $CH_2$), 3.35 (t, 2H, $NCH_2$); $^{31}$P, $\delta$ 35.8 (s); $^{13}$C, $\delta$ 11.4 ($CH_3$), 21.3 ($CH_2$), 49.3 ($NCH_2$), 159.9 (t, NCN, $^2J_{C-P}$ = 10.4 Hz). MS (EI) [*m/e*, (species), intensity]: 358 ($M^+$) 7; 343 ($M^+ - CH_3$) 3; 329 ($M^+ - C_2H_5$) 100; 258 [$M^+ - N(C_3H_7)_2$] 41. Anal. Calcd for $C_7H_{14}Cl_4N_4P_2$: C, 23.49; H, 3.91; N, 15.66. Found: C, 23.83; H, 3.80; N, 15.25.

**Hydrolysis of 8.** The hydrolytic behavior of *N*,*N*′-dimethylamino-substituted dicarbaphosphazenes is investigated by the addition of 1 equiv of water as an emulsion in chloroform to **8**. The spectral data obtained for the hydrolyzed product, $Cl(O)PN(H)N_2C_2[N(C_2H_5)_2]_2$ (**11**), are as follows. IR ($cm^{-1}$): 3400 ms, v br, 1607 s, 1573 vs, 1532 ms, 1490 sh, 1462 s, 1378 ms, 1356 s, 1316 m, 1283 s, 1252 ms, 1220 mw, 1178 mw, 1098 m, 1081 m, 1032 mw, 1002 m, 957 ms, 920 m, 844 mw, 793 mw, 763 m, 731 ms, 647 mw. NMR: $^1$H, $\delta$ 1.15 (t, 12H, $CH_3$), 3.40 (m, 8H, $NCH_2$), 9.3 (s, br, 1H, HN); $^{31}$P, $\delta$ 10.9 (s); $^{13}$C, $\delta$ 11.87, 12.30 ($CH_3$), 43.02, 43.72 ($NCH_2$), 151.66, 151.71 (d, NCN, $^2J_{C-P}$ = 3.6 Hz). X-ray diffraction quality crystals are obtained by recrystallization from a chloroform/hexane mixture.

**Reactions of $N_3PC_2Cl_4$ with $[(LiOCH_2CF_2)_2(CF_2)_n]$ ($n$ = 0 or 1).** A solution of $(HOCH_2CF_2)_2(CF_2)_n$ ($n$ = 0 or 1) (~12.6 mmol) in ~20 mL of diethyl ether is placed in a 100 mL three-necked flask equipped with a magnetic stir bar, a reflux condenser, and a nitrogen inlet. After cooling of the flask to −78 °C, a slight excess of *n*-butyllithium (10 mL, 2.5 M in hexanes) is slowly introduced by syringe, and the reaction mixture is then stirred for 4 h as the bath warms to 25 °C. The contents are recooled to −78 °C, and a solution of $N_3PC_2Cl_4$ (12.5 mmol) in ~30 mL of diethyl ether is transferred into the reaction flask *via* a cannula. The reaction mixture is slowly allowed to warm to 25 °C and then refluxed gently overnight. Filtration followed by solvent removal under vacuum affords a dirty white solid characterized to be $(CF_2)_n(CF_2CH_2O)_2PNC_2Cl_2$ (yield 81−87%, $n$ = 0; 55−60%, $n$ = 1). The crude product is then purified by sublimation under vacuum (0.03 Torr) at 120−150 °C.

**Properties of $(CF_2CH_2O_2)PN_3C_2Cl_2$ (12).** $(CF_2CH_2O)_2PN_3C_2Cl_2$ is obtained as a colorless crystalline solid (mp 131 °C). The spectral data obtained for this compound are as follows. IR ($cm^{-1}$): 1563 sh, 1545 vs, 1464 vs, 1375 vs, 1314 vs, 1292 ms, 1265 sh, 1245 m, 1201 w, 1175 m, 1157 ms, 1139 s, 1076 vs, 1047 s, 1025 ms, 922 m, 905 m, 878 ms, 780 ms, 736 m, 709 mw, 672 ms. NMR: $^1$H, $\delta$ 4.61 (m, $OCH_2$); $^{19}$F, $\delta$ −127.60 (s, $CF_2$); $^{31}$P, $\delta$ 28.95 (pentet, $^3J_{P-H}$ = 17.6 Hz); $^{13}$C, $\delta$ 62.8 (tm, $CH_2$), 112.2 (tt, $CF_2$, $^1J_{C-F}$ = 287 Hz, $^2J_{C-F}$ = 29 Hz,), 172.2 (d, NCN, $^2J_{C-P}$ = 11 Hz). MS (EI) [*m/e*, (species), intensity]: 327 ($M^+$) 49; 292 ($M^+ - Cl$) 100. Anal. Calcd for $C_6H_4Cl_2F_4N_3O_2P$: C, 21.95; H, 1.22; N, 12.81. Found: C, 21.78; H, 1.22; N, 12.76.

**Properties of $[CF_2(CF_2CH_2O)_2]PN_3C_2Cl_2$ (13).** $[CF_2(CF_2CH_2O)_2]PN_3C_2Cl_2$ is obtained as a colorless crystalline solid upon sublimation. The spectral data obtained for this compound areas follows. IR ($cm^{-1}$): 1565 m, 1551 m, 1536 m, 1462 vs, 1377 vs, 1342 m, 1312 vs, 1263 m, 1245 m, 1168 vs, 1135 s, 1086 vs, 1068 vs, 990 mw, 940 m, 918 mw, 904 m, 877 m, 785 ms, 729 m, 709 mw, 644 w, 620 m, 603 m. NMR: $^1$H, $\delta$ 4.7 (m, $OCH_2$); $^{19}$F, $\delta$ −117.1 (m, 4F, $CH_2CF_2$), −127.60 (s, 2F, $CF_2$); $^{31}$P, $\delta$ 27.8 (pentet, $^3J_{P-H}$ = 15.4 Hz); $^{13}$C, $\delta$ 63.9 (m, $CH_2$), 111.0 (tt, $CH_2CF_2$, $^1J_{C-F}$ = 267 Hz, $^2J_{C-F}$ = 28.9 Hz,), 113.4 (tm, $-CF_2CF_2-$, $^1J_{C-F}$ = 260 Hz, $^2J_{C-F}$ = 28.2 Hz), 172.4 (d, NCN, $^2J_{C-P}$ = 11.3 Hz). MS (EI) [*m/e*, (species), intensity]: 377 ($M^+$) 40; 358 ($M^+ - F$) 2; 342 ($M^+$ - Cl) 77.6.

**Reaction of $N_3P_2C_2Cl_4$ with $[(LiOCH_2CF_2)_2]$.** This reaction is carried out in a manner similar to that described above. However, a mixture of monospiro $(CF_2CH_2O)_2P_2N_3CCl_3$ (**14**) and dispiro $(CF_2CH_2O_2)_2P_2N_3CCl$ (**15**) carbaphosphazenes is formed regardless of the reactant stoichiometry (the relative ratio of **14:15** is 1:~0.25). Our attempts to separate **14** and **15** by vacuum sublimation were not successful as both of these compounds are found to sublime at similar temperatures (100−120 °C)/0.05 Torr. These two compounds can easily be identified from the $^{31}$P NMR. The spectral data for the mixture

(54) *Aldrich library of 1H and 13C FT NMR*; Pouchert, C. J., Behnke, J., Eds.; Aldrich Chemical Co.: Milwaukee, WI, 1993.

are as follows. IR ($cm^{-1}$): 1592 m, 1523 m, 1461 vs, 1377 vs, 1304 s, 1285 s, 1240 s, 1199 ms, 1147 vs, 1111 s, 1073 vs br, 983 mw, 956 mw, 926 ms, 864 ms, 838 ms, 788 w, 743 m, 708 m, 672 ms. NMR: $^1$H, $\delta$ 4.4−4.6 (m, $OCH_2$); $^{19}$F, $\delta$ −127.60 (s, $CF_2$); $^{31}$P, $\delta$ 17.3 (dp, $P_{monospiro}$, $^2J_{P-P}$ = 67.3 Hz, $^3J_{P-H}$ = 16.8 Hz), 22.7 (m, $P_{dispiro}$), 40.9 (d, $P_{P-Cl}$); $^{13}$C, $\delta$ 62.5 (m, $CH_2$), 112.36 (tt, $CH_2CF_2$, $^1J_{C-F}$ = 258 Hz, $^2J_{C-F}$ = 28.4 Hz,), 168.8, 170.0 (t, $NCN_{spiro}$, $^2J_{C-P}$ = 15.2, 15.0 Hz). MS (EI) [*m/e*, (species), intensity]: 471 ($M_{dispiro}^+$) 16; 436 ($M_{dispiro}^+$ − Cl) 77; 381 ($M_{monospiro}^+$) 87; 346 ($M_{monospiro}^+$ − Cl) 100.

**Substitution Reactions of $[(CF_2)_n(CF_2CH_2O)_2]PN_3C_2Cl_2$ ($n$ = 0 or 1). (i)Substitution reactions with 4-$FC_6H_4XNa$ (X = O or S).** A suspension of 15 mmol of NaH in ∼20 mL of diethyl ether is added to a 100 mL three-necked flask fitted with a reflux condenser, a nitrogen inlet, and a rubber septum. To this is added dropwise a solution of 4-$FC_6H_4SH$ (14 mmol) in 10 mL of the same solvent. The reactants are stirred vigorously for about 3 h and then cooled to −78 °C. A solution of compound **12** (7 mmol in ∼ 40 mL of diethyl ether) is then transferred into the reaction flask *via* a cannula. The reaction mixture is slowly allowed to warm to 25 °C over a period of 4 h and then refluxed gently for 12 h. Filtration followed by removal of the solvent under vacuum affords a dirty white solid material, which is crystallized from a mixture of hexane/chloroform. The reaction of 4-$FC_6H_4OH$ is carried out similarly.

**Properties of $(CF_2CH_2O)_2PN_3C_2(4\text{-}FC_6H_4O)_2$ (16).** $(CF_2CH_2O)_2PN_3C_2(4\text{-}FC_6H_4O)_2$ is obtained as a white solid (mp 144−146 °C) in 78% yield. The spectral data for this compound are as follows. IR ($cm^{-1}$): 1657 sh, 1611 s, 1566 s, 1504 s, 1461 vs, 1413 s, 1376 vs, 1285 m, 1242 s, 1191 vs, 1145 vs, 1106 vs, 1074 vs, 1013 m, 983 ms, 922 m, 910 m, 865 m, 847 ms, 833 m, 815 mw, 780 mw, 759 w, 744 vw, 725 w, 708 w, 671 ms. NMR: $^1$H, $\delta$ 4.4 (m, 4H, $OCH_2$), 6.96 (br s, 8H, $FC_6H_4O$); $^{19}$F, $\delta$ −117.1 (m, 2F, $OC_6H_4F$), −127.8 (s, 4F, $CF_2$); $^{31}$P, $\delta$ 42.7 (pentet, $^3J_{P-H}$ = 17.2 Hz); $^{13}$C, $\delta$ 61.9 (tm, $OCH_2$), 112.4 (tt, $CF_2$, $^1J_{C-F}$ = 258 Hz, $^2J_{C-F}$ = 29 Hz), 115.7 (d, $C_m$, $^2J_{C-F}$ = 24), 123.1 (d, $C_o$, $^3J_{C-F}$ = 8 Hz), 147.3 (s, $C_{ipso}$), 160.2 (d, $C_pF$, $^1J_{C-F}$ = 244 Hz), 172.6 (d, NCN, $^2J_{C-P}$ = 19.4 Hz); MS (EI) [*m/e*, (species), intensity]: 368 ($M^+$ - $OC_6H_4F$) 100. MS (CI) 480 ($M^+$ + 1) 9; 460 ($M^+$ − F) 9; 368 ($M^+$ − $OC_6H_4F$) 100.

**Properties of $(CF_2CH_2O)_2PN_3C_2(4\text{-}FC_6H_4S)_2$ (17).** $(CF_2CH_2O)_2PN_3C_2(4\text{-}FC_6H_4S)_2$ is obtained as a pale yellow crystalline solid (mp 153−154 °C). The spectral data for this compound are as follows. IR ($cm^{-1}$): 1593 s, 1494 vs, 1475 vs br, 1401 m, 1358 vs, 1338 vs, 1292 s, 1281 s, 1236 s, 1209 s, 1148 vs, 1081 vs, 1052 vs, 1026 ms, 1015 m, 935 mw, 922 s, 896 ms, 863 s, 829 vs, 806 mw, 791 ms, 774 m, 723 m, 708 m, 671 ms, 638 mw. NMR: $^1$H, $\delta$ 4.3 (m, 4H, $CH_2$), 6.97 (t, 4H, $ArH_{meta}$), 7.37 (m, 4H, $ArH_{ortho}$); $^{19}$F, $\delta$ −111.0 (m, 2F, $SC_6H_4F$), −127.6 (s, 4F, $CF_2$); $^{31}$P, $\delta$ 26.7 (pentet, $^3J_{P-H}$ = 17.2 Hz); $^{13}$C, $\delta$ 61.8 (tm, $CH_2$), 112.3 (tt, $CF_2$, $^1J_{C-F}$ = 258 Hz, $^2J_{C-F}$ = 28 Hz,), 116.0 (d, $C_m$, $^2J_{C-F}$ = 22.3), 137.3 (d, $C_o$, $^3J_{C-F}$ = 9.1 Hz), 123.5 (s, $C_{ipso}$), 131.3 (d, NCN, $^2J_{C-P}$ = 8.4 Hz), 163.5 (d, $C_pF$, $^1J_{C-F}$ = 250.3 Hz); MS (EI) [*m/e*, (species), intensity]: 511 ($M^+$) 88; 492 ($M^+$ − F) 31; 384 ($M^+$ − $SC_6H_4F$) 63. Anal. Calcd for $C_{18}H_{12}F_6N_3O_2PS_2$: C, 42.27; H, 2.34; N, 8.23. Found: C, 42.23; H, 2.49; N, 8.08.

**(ii) Substitution Reactions with $(CH_3)_3SiN(CH_3)_2$.** A 50-mL round-bottomed flask, equipped with a Kontes Teflon stopcock, is loaded with **12** (1.15 g, 3.5 mmol) and then evacuated at −196 °C. Methylene chloride (∼20 mL) and $(CH_3)_3SiN(CH_3)_2$ (8 mmol) are then transferred under vacuum into the reaction flask. The reaction flask is then allowed to warm to 25 °C, filled with nitrogen gas, and attached to a reflux condenser. The contents are then refluxed at 40 °C for 12 h with stirring under an inert atmosphere. Removal of all volatile material under vacuum affords a pale-yellowish solid in ∼85−90% yield, which is further purified by recrystallization from a mixture of chloroform/cyclohexane. Compound **13** is reacted similarly.

**Properties of $(CF_2CH_2O)_2PN_3C_2[N(CH_3)_2]_2$ (18).** $(CF_2CH_2O)_2PN_3C_2[N(CH_3)_2]_2$ is obtained as a colorless crystalline solid (mp 190−192 °C). The spectral data obtained for this compound are as follows. IR ($cm^{-1}$): 1561 ms, 1517 s, 1464 vs, 1405 s, 1375 vs, 1291 m, 1275 m, 1239 ms, 1142 vs, 1105 vs, 1088 vs, 1069 s, 992 s, 946 ms, 926 ms, 829 ms, 766 m, 766 m, 712 m, 671 ms, 611 ms. NMR: $^1$H, $\delta$ 3.0 [br s, 12H, $N(CH_3)_2$], 4.35 (m, 4H, $CH_2$); $^{19}$F, $\delta$ −127.6 (s, $CF_2$); $^{31}$P, $\delta$ 40.0 (pentet, $^3J_{P-H}$ = 16.5 Hz); $^{13}$C, $\delta$ 36.1 (s), 36.5 (s) [$N(CH_3)_2$]; 61.1 (tm, $CH_2$), 113.1 (tt, $CF_2$, $^1J_{C-F}$ = 255 Hz, $^2J_{C-F}$ = 28 Hz), 165.8 (d, NCN, $^2J_{C-P}$ = 18.2 Hz). MS (EI) [*m/e*, (species), intensity]: 345 ($M^+$) 100; 330 ($M^+$ − $CH_3$) 36; 301 [$M^+$ − $N(CH_3)_2$] 63. Anal. Calcd for $C_{10}H_{16}F_4N_5O_2P$: C, 34.78; H, 4.63. Found: C, 33.54; H, 4.45.

**Properties of $[CF_2(CF_2CH_2O)_2]PN_3C_2[N(CH_3)_2]_2$ (19).** $[CF_2(CF_2CH_2O)_2]PN_3C_2[N(CH_3)_2]_2$ is obtained as a colorless crystalline solid upon sublimation (mp 116−119 °C). The spectral data obtained for this compound are as follows. IR ($cm^1$): 1572 ms, 1528 s, 1401 s, 1305 sh, 1275 m, 1216 ms, 1151 vs, 1128 vs, 1115 s, 1088 vs, 1054 vs, 1007 s, 996 s, 945 s, 933 m, 917 ms, 841 ms, 799 ms, 761 m, 732 w, 708 mw, 630 ms, 614 ms. NMR: $^1$H, $\delta$ 3.1 [br s, 12H, $N(CH_3)_2$], 4.5 (m, 4H, $CH_2$); $^{19}$F, $\delta$ −116.8 (m, 4F, $CH_2CF_2$), −125.2 (br s, 2F, $CF_2$); $^{31}$P, $\delta$ 39.2 (pentet, $^3J_{P-H}$ = 15.2 Hz); $^{13}$C, $\delta$ 36.1 (s), 36.5 (s) [$N(CH_3)_2$]; $\delta$ 62.8 (tm, $CH_2$), 111.4 (ttm, $CH_2CF_2$, $^1J_{C-F}$ = 234 Hz, $^2J_{C-F}$ = 28 Hz), 114.4 (tt, $-CF_2CF_2-$, $^1J_{C-F}$ = 259 Hz, $^2J_{C-F}$ = 27 Hz), 165.6 (d, NCN, $^2J_{C-P}$ = 18.4 Hz). MS (EI) [*m/e*, (species), intensity]: 395 ($M^+$) 100; 380 ($M^+$ − $CH_3$) 45; 351 [$M^+$ − $N(CH_3)_2$] 65. Anal. Calcd for $C_{11}H_{16}F_6N_5O_2P$: C, 33.42; H, 4.08. Found: C, 33.85; H, 4.26.

**Acknowledgment.** We are grateful to the National Science Foundation (CHE-9310389, NSF-EPSCoR OSR-9350539) and the Air Force Office of Scientific Research (91-0189) for support of this research. The single-crystal CCD X-ray facility at the University of Idaho was established with the assistance of the NSF−Idaho EPSCoR program under NSF OSR-9350539 and the M. J. Murdock Charitable Trust, Vancouver, WA. Dr. R. J. Staples (University of Idaho) is thanked for his helpful assistance during the X-ray diffraction studies. We also thank Dr. Gary Knerr for obtaining the mass spectral data and assistance in high-temperature NMR experiments.

**Supporting Information Available:** For compounds **1**, **2**, **7**, **9**−**14** and **16**−**19**, tables listing full data collection and processing parameters, bond lengths and angles, atomic coordinates, equivalent isotropic and anisotropic displacement coefficients, and hydrogen atom coordinates and isotropic displacement coefficients (74 pages). Ordering information is given on any current masthead page.

IC9612921